AD-A073 330 SRI INTERNATIONAL MENLO PARK CA F/G 17/5
LIDAR OBSERVATIONS AT 0.7-MICROMETERS AND 10.6-MICROMETERS WAVE--ETC(U)
JUL 79 J E LAAN DAAG29-77-C-0001
UNCLASSIFIED SRI-TR-3 ARO-13833.4-GS NL

| OF |
AD
A073330

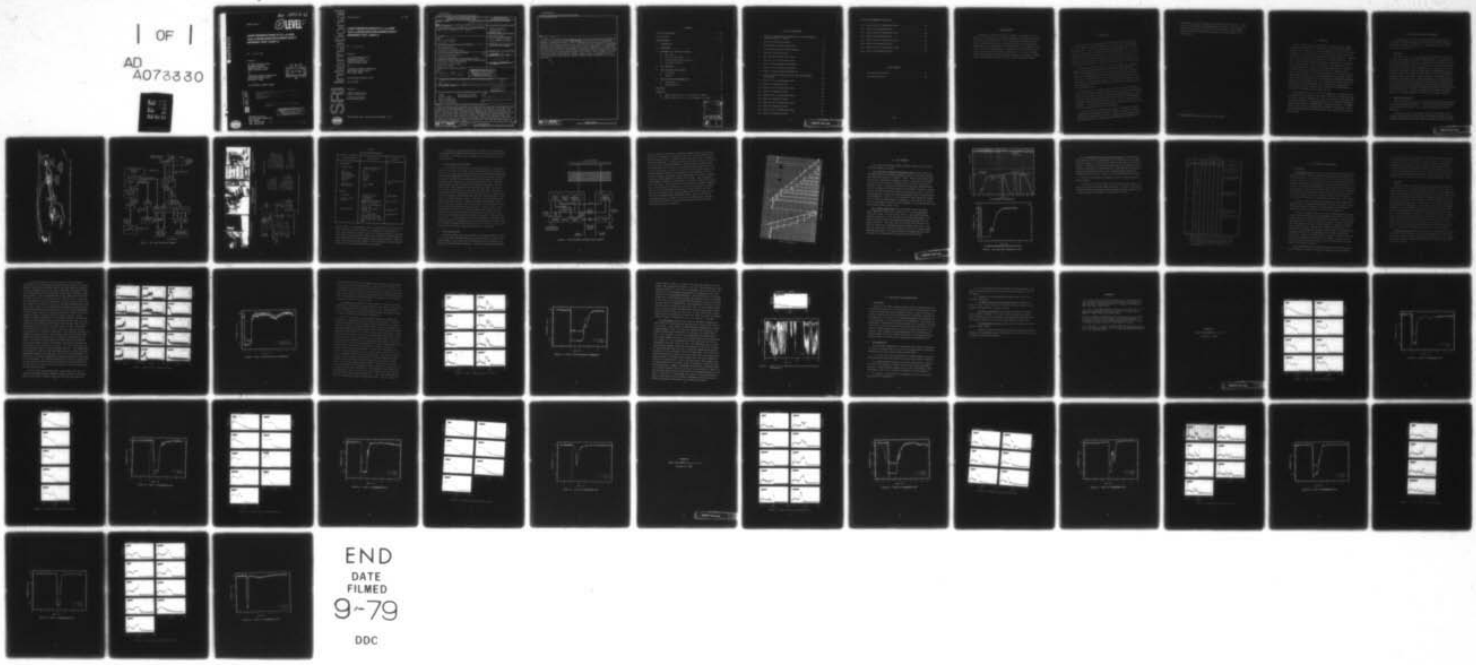

END
DATE
FILMED
9-79
DDC

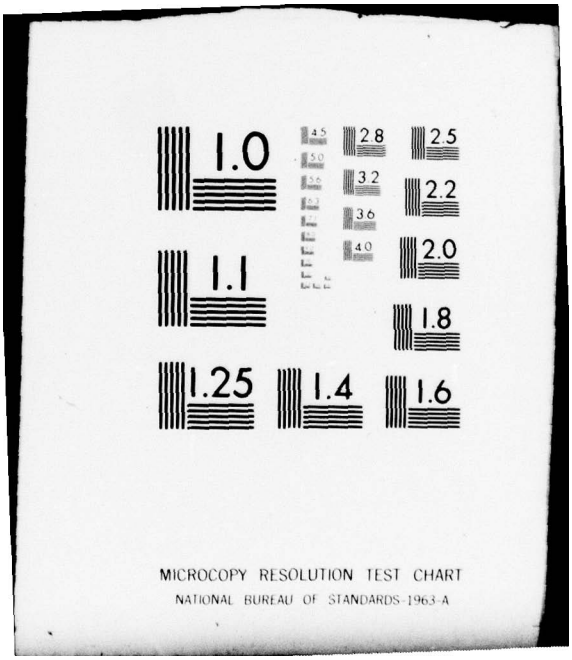
1.0
1.1
1.25
1.4
1.6
1.8
2.0
2.2
2.5
2.8
3.2
3.6
4.0
4.5
5.0
5.6
MICROCOPY RESOLUTION TEST CHART
NATIONAL BUREAU OF STANDARDS-1963-A

ARO 13833.4-GS

(11) LEVEL II

Technical Report 3

LIDAR OBSERVATIONS AT 0.7-μm AND 10.6-μm WAVELENGTHS DURING DUSTY INFRARED TEST I (DIRT-I)

By: J. E. van der LAAN

Prepared for:

U.S. ARMY RESEARCH OFFICE
GEOSCIENCES DIVISION
RESEARCH TRIANGLE PARK
NORTH CAROLINA 27709

and

ATMOSPHERIC SCIENCES LABORATORY
WHITE SANDS MISSILE RANGE
NEW MEXICO 88002

ARO CONTRACT DAAG29-77-C-0001

Approved for public release; distribution unlimited.

333 Ravenswood Avenue
Menlo Park, California 94025 U.S.A.
(415) 326-6200
Cable: SRI INTL MNP
TWX: 910-373-1246

SRI International

Technical Report 3

July 1979

LIDAR OBSERVATIONS AT 0.7-μm AND 10.6-μm WAVELENGTHS DURING DUSTY INFRARED TEST I (DIRT-I)

By: J. E. van der LAAN

Prepared for:

U.S. ARMY RESEARCH OFFICE
GEOSCIENCES DIVISION
RESEARCH TRIANGLE PARK
NORTH CAROLINA 27709

and

ATMOSPHERIC SCIENCES LABORATORY
WHITE SANDS MISSILE RANGE
NEW MEXICO 88002

ARO CONTRACT DAAG29-77-C-0001

SRI Project 5862

Approved by:

WARREN B. JOHNSON, *Director*
Atmospheric Sciences Laboratory

CHARLES A. SHOENS, *Director*
Systems Techniques Laboratory

333 Ravenswood Avenue • Menlo Park, California 94025 • U.S.A.

SRI International

UNCLASSIFIED

SECURITY CLASSIFICATION OF THIS PAGE (When Data Entered)

REPORT DOCUMENTATION PAGE

READ INSTRUCTIONS BEFORE COMPLETING FORM

1. REPORT NUMBER (6)

2. GOVT ACCESSION NO. micrometers

3. RECIPIENT'S CATALOG NUMBER

4. TITLE (and Subtitle)
LIDAR OBSERVATIONS AT 0.7-μm AND 10.6-μm WAVELENGTHS DURING DUSTY INFRARED TEST I (DIRT-I),

5. TYPE OF REPORT & PERIOD COVERED
Technical Report 3
Covering the Period
October 1978

6. PERFORMING ORG. REPORT NUMBER
SRI Project 5862

7. AUTHOR(s)
(10) Jan E. van der Laan

8. CONTRACT OR GRANT NUMBER(s)
Contr. DAAG29-77-C-0001 (15)

9. PERFORMING ORGANIZATION NAME AND ADDRESS
SRI International
333 Ravenswood Avenue
Menlo Park, California 94025

10. PROGRAM ELEMENT, PROJECT, TASK AREA & WORK UNIT NUMBERS

11. CONTROLLING OFFICE NAME AND ADDRESS (11)
U.S. Army Research Office
Geosciences Division
Research Triangle Park, North Carolina 27709

12. REPORT DATE
July 1979

13. NO. OF PAGES
65

15. SECURITY CLASS. (of this report)
(12) 58 p.

14. MONITORING AGENCY NAME & ADDRESS (if diff. from Controlling Office)
Atmospheric Sciences Laboratory
White Sands Missile Range
New Mexico, 88002

15a. DECLASSIFICATION/DOWNGRADING SCHEDULE

16. DISTRIBUTION STATEMENT (of this report)
(14) SRI-TR-3

DISTRIBUTION STATEMENT A
Approved for public release; Distribution Unlimited

17. DISTRIBUTION STATEMENT (of the abstract entered in Block 20, if different from report)
(9) Rept. for period ending oct 78,

18. SUPPLEMENTARY NOTES
(18) ARO

19. KEY WORDS (Continue on reverse side if necessary and identify by block number)
LIDAR
Military smoke
Optical properties
Optical backscatter
Optical transmission
Dense dust and smoke
Multiwavelength lidar
(19) 13833.1-GS
micrometers

20. ABSTRACT (Continue on reverse side if necessary and identify by block number)
This technical report describes lidar measurements and results using the U.S. Army Atmospheric Sciences Laboratory's 10.6-μm lidar and the SRI Mark IX (0.7-μm) lidar systems during the Dusty Infrared Test-I (DIRT-I). The test was conducted at the White Sands Missile Range in October 1978. Transmission comparisons are made between the two wavelengths with artillery barrages, TNT explosions, and oil/rubber fire-generated dust and smoke clouds in a test zone midway (1 km) along the lidar path. A target at the end of the lidar path provided a reference backscatter return for the transmission measurements. Backscatter properties of the dust and smoke clouds are also discussed. —next page

DD FORM 1 JAN 73 1473
EDITION OF 1 NOV 65 IS OBSOLETE

UNCLASSIFIED
SECURITY CLASSIFICATION OF THIS PAGE (When Data Entered)

SECURITY CLASSIFICATION OF THIS PAGE (When Data Entered)

19. KEY WORDS (Continued)

20. ABSTRACT (Continued)

Results of the DIRT-I program indicate that the broad particle size distribution present in the dust generated ~~at White Sands~~ produced little if any wavelength dependent transmission effects. The few observed exceptions where greater 10.6-μm transmission is indicated generally can be explained by the presence of wavelength-dependent smoke along the optical path, which is also generated by the detonations. Backscatter-to-transmission relationships are grossly related but, in general, are quite nonlinear, as can be expected when multiple and specular scatter by the large particles, as well as strong attenuations, are involved. The oil/rubber fire generated dense black smoke that was totally opaque to the 0.7 μm lidar, while the 10.6 μm transmission measurements indicate a "worse-case" transmission of approximately 6%.

micrometers

micrometers

CONTENTS

LIST OF ILLUSTRATIONS

LIST OF ILLUSTRATIONS (Continued)

LIST OF TABLES

ACKNOWLEDGMENTS

The author is indebted to Bruce W. Kennedy, test conductor of the DIRT-I test program, for his excellent handling of the field program and for his special consideration of lidar requirements without which the lidar system characterizations would have been less than satisfactory. Additionally, the author wishes to acknowledge Dr. J. S. Randhawa of ASL for his work in coordinating lidar activities during the field program and Mr. K. Ballard for operational assistance. Dr. E. Uthe of SRI provided helpful suggestions and assistance throughout the program. Norman Nielsen and Rod March operated the lidar systems during the program.

I INTRODUCTION

Two-wavelength lidar measurements were made during the Dusty Infrared Test I (DIRT-I) program conducted at White Sands Missile Range (WSMR) in October 1978. The U.S. Army Atmospheric Science Laboratory's 10.6-μm wavelength lidar system (ASL-lidar) and SRI International's 0.7-μm ruby lidar system (MK-IX) were operated over a common 2-km optical path during the DIRT-I test. Static TNT charges, artillery rounds, live artillery barrages, and an oil/rubber fire generated dust and smoke clouds in a test zone midway (1 km) between the lidar systems and a beam-stop lidar target.

Primary lidar backscatter data for both wavelengths were recorded on magnetic tape using the Mark IX lidar data system while independent 10.6-μm lidar transmission data were recorded on strip chart in the ASL lidar van. Photographs were also taken every 30 to 60 seconds during each event of range-resolved 10.6-μm backscatter amplitude data (A-scope presentations). TV video recordings of the lidar optical path were also taken during the DIRT-I events for safety, additional documentation, and as an operational aid.

In this report, an outline of the two systems and the two-system interface will first be presented, followed by a discussion of operation, data, and processing required to derive transmission comparisons. Selected events will be discussed in detail in the text, and two-wavelength comparison data for each event on the last two days of testing will be appended. In addition, ASL lidar backscatter photographs and strip chart data for the earlier events will be discussed.

It should be noted that while this report is primarily a DIRT-I program lidar data report and review, a major objective of the lidar participation during this test was to evaluate the performance of the ASL lidar system and to examine multiwavelength lidar techniques for

measurements of optical properties of battlefield dust and smoke. Therefore, the conclusions and recommendations at the end of this report will address these objectives as well as the data results. Documentation regarding the ASL lidar has been submitted as Technical Report 21* on this contract.

* References are listed at the end of this report.

II BACKGROUND

Recent military interest in methods to measure real-time, three-dimensional distributions of density and optical parameters of dense smoke and dust clouds led to a two-wavelength (0.7-μm and 10.6-μm) lidar experiment to collect basic data on generated smoke clouds. The first experiment was conducted at Dugway Proving Grounds in late 1977. Results of this initial experiment are reported in Technical Report No. 1[2] on this contract and were generally consistent with theoretical data relating to aerosol particle-size distributions. The Dugway test clearly illustrated both the usefulness of long-wavelength lidar for detection of large particle-size aerosols and its ability to penetrate small particle-size aerosols. The encouraging results of this first two-wavelength lidar field test led to the construction of an improved 10.6-μm lidar system, the ASL lidar, which incorporated recommended improvements resulting from the Dugway tests. The construction of the ASL lidar was completed in time to participate in the scheduled field programs at White Sands, New Mexico (DIRT-I October 1978) and the SMOKE WEEK-II in November 1978 at Eglin Air Force Base, Florida.

The primary objective of the DIRT-I program is to evaluate various techniques to measure physical and optical properties of battlefield dust. The lidar technique represents one of the most promising techniques being evaluated by the ASL. Following the DIRT-I test the ASL and SRI MARK IX lidars participated in the SMOKE-WEEK-II program in Florida. The SMOKE-WEEK-II data, which were gathered under funding by ASL and ARO, are now being evaluated and will be included in the final report on this current ARO contract.

III EQUIPMENT AND OPERATING PROCEDURE

The following descriptions outline the equipment and procedures used during the DIRT-I program; the illustration in Figure 1 indicates the general experimental configuration. A detailed site description may be found in Reference 3.

A. ASL Lidar

The ASL lidar is a 10.6-μm wavelength system which is installed in the ASL's laser Doppler velocimeter (LDV) laser van. Specifications for the system are given in Table 1 and a detailed system description can be found in Technical Report No. 2[1] on this contract. Basically the system is made up of two major system components: (1) a pulsed CO_2 laser that generates a very short, high peak power IR pulse transmission, and (2) a narrow field-of-view optical receiver that collects the backscattered energy and directs the signal to an IR detector. After detection and logarithmic amplification, the signal is digitized by a high-speed transient recorder which provides range-resolved backscatter amplitude data output in both digital and digitally-reconstructed analog (DAC) formats. The digital output is primarily intended for recording and processing use while the DAC output is useful in observing the real-time backscatter returns. A functional diagram of the ASL lidar is shown in Figure 2.

B. Mark IX Lidar System

The Mark IX lidar system is a self-contained mobile system operating at the ruby wavelength of 0.6943 μm. Details of the system and specifications are shown in Figure 3 and a complete description is given in Reference 4.

A principal feature of the Mark IX system is its digital data recording, processing, and display system for real-time viewing of range-resolved backscatter data in both A-scope and range-time-intensity (RTI)

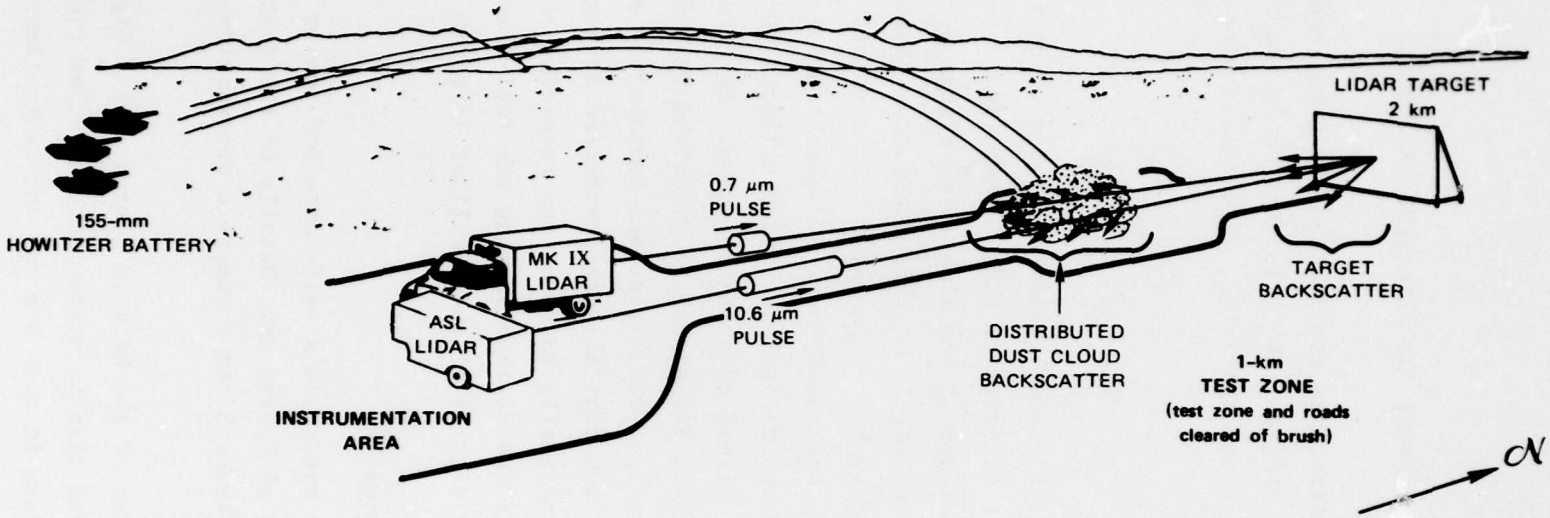

FIGURE 1 EXPERIMENTAL CONFIGURATION FOR TWO-WAVELENGTH LIDAR OBSERVATIONS — DIRT-1

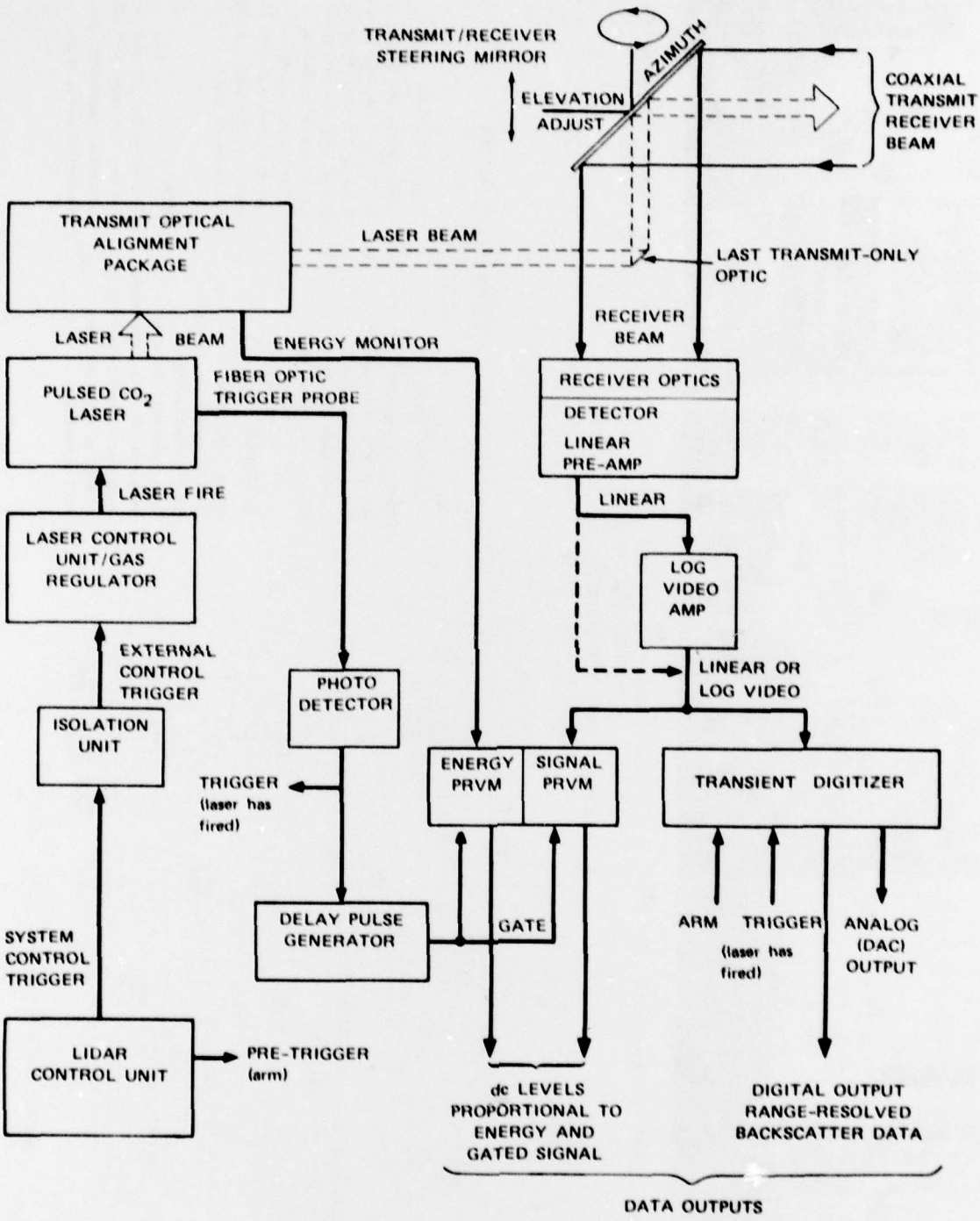

FIGURE 2 ASL LIDAR FUNCTIONAL DIAGRAM

(a) MARK IX LIDAR VAN

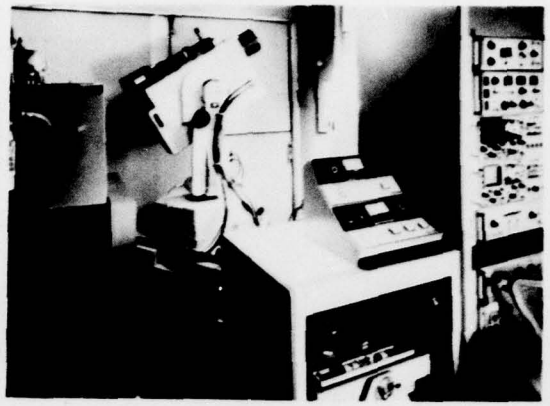

(b) ANALOG DATA AND FIRE CONTROL ELECTRONICS

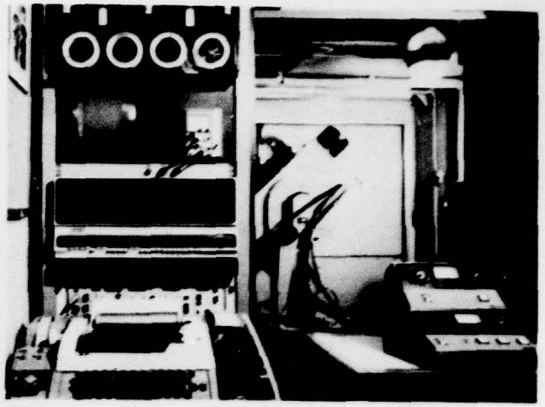

(c) DIGITAL DATA ELECTRONICS AND TV DISPLAY

EXTERIOR AND INTERIOR VIEWS OF THE LIDAR VAN

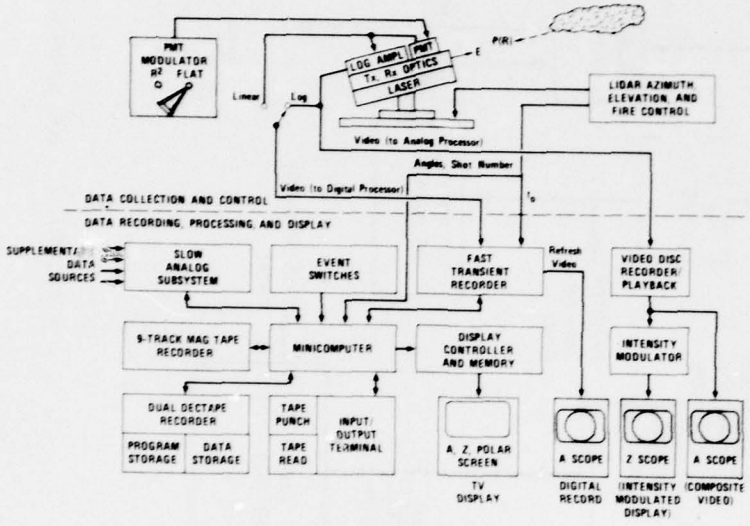

BLOCK DIAGRAM OF THE LIDAR SYSTEM

LIDAR SPECIFICATIONS

TRANSMITTER

6943Å Wavelength
0.5 mrad Beamwidth
1.0 J Pulse Energy
30 ns Pulse Length
60 ppm Maximum PRF

RECEIVER

6 inch Newtonian
1 to 5 mrad Field of View
5Å Predetection Filter
RCA 7265 PMT Detector
4-decade, 35-MHz Logarithmic Amplifier. Inverse-range-squared or step-function PMT modulation.

DATA SYSTEMS

Analog video disc recording (4.5 MHz) with A-scope and Z-scope real-time displays. Digital magnetic tape (data and programs) recording (25 MHz) with computer processing and real-time TV display (512 x 256 x 4 bit) of processed data.

MOUNT

Automatic azimuth and elevation fire and scan with 0.1° minimum resolution. Automatic reset. Mechanical safety stops.

FIGURE 3 THE SRI MARK IX MOBILE LIDAR SYSTEM

Table 1

ASL LIDAR SPECIFICATIONS

System Component	Specification	Comments
Transmitter		
Manufacturer	Lumonics Research Ltd., Model TEA-101-2	
Type	CO_2	
Wavelength	10.6 μm	
Beam diameter	3.1 cm	
Beam divergence	1.2 mrad	
Operation	pulsed	
Energy	250 mJ	No nitrogen gas mix
Pulsewidth	75 ns (FWHM)	
PRF (maximum)	1 pps	
Receiver		
Telescope	12-inch (30 cm), Newtonian	LDV primary
Field of view	1.23 mrad	
Detector	Honeywell Associates; HgCdTe photodiode; $D^* = 1.3 \times 10^{10}$ cmHz$^{\frac{1}{2}}$W^{-1}; 100 MHz BW	LN_2-cooled
Postamplifier	Linear: 26 dB gain, 100 MHz BW	Appendix G[1]
	Log: tangential sensitivity -111 dBr; ±0.5 dB linearity over 80-dB range; 15-ns rise time	Appendix H[1]

presentations. The recorded data can be processed after the event on the Mark IX system's computer (PDP-11) or reformatted for processing on a large, more versatile computer system. The latter processing is preferred since there is generally only enough time to perform spot-check analysis in the field due to the large amount of data collected during a field program. Also, more efficient software can be utilized on a larger machine and more useful plotting peripherals are available.

In addition to recording lidar data, the Mark IX is equipped with an integrating nephelometer that measured the in situ aerosol scattering coefficient. This data is also recorded on the data system for post-event analysis.

C. Two-Wavelength Lidar Interface

The current ASL lidar system is not equipped with a recording capability as its associated computer van is being utilized on other ASL programs. To provide a processing capability during the DIRT-I program and the following SMOKE-WEEK-II program, the ASL lidar backscatter data were recorded on the Mark IX lidar data system on an alternate record basis with backscatter signatures produced by the Mark IX lidar. The block diagram shown in Figure 4 details the interface connections. The ASL lidar control unit provides the lidar firing rates while interface control signals are developed by a two-lidar interface unit. Basically, an ASL lidar control signal (pre-trig pulse) is sent to the lidar interface unit located in the Mark IX lidar van; here control signals are generated to prepare the data system to accept ASL lidar backscatter data. When the ASL lidar "fires" it sends a "laser has fired" pulse to the Mark IX transient recorder, and a 10.6-μm (ASL lidar) backscatter record is digitized and recorded on nine-track tape. The lidar interface unit then generates a second set of control signals that prepare the data system to accept a 0.7-μm (Mark IX) backscatter record and also sends a fire pulse to the Mark IX ruby fire-control electronics. When the ruby laser fires, a 0.7-μm backscatter record is digitized and recorded. This sequence of events is repeated for each control signal from the ASL lidar. For the DIRT-I program the firing rate was set for every 2 s with a 0.5-s delay between the 10.6 μm lidar firing and the 0.7 μm firing.

D. Operating Procedure

The general lidar operating procedure used during the DIRT-I program was to start lidar operation prior to an event in order to record a sufficient amount of pre-event data to establish reference conditions for backscatter and transmission analysis. Operation would continue through

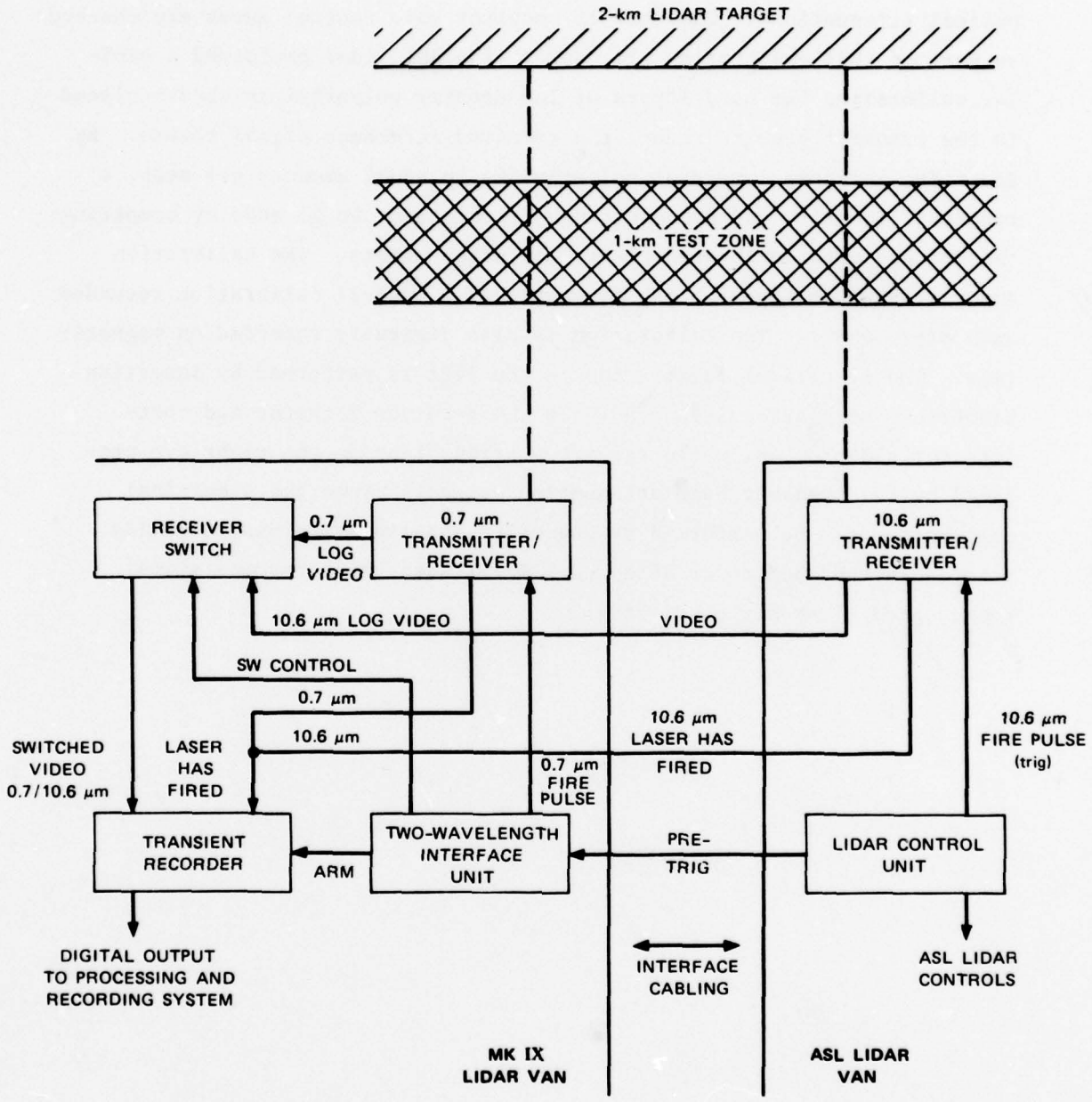

FIGURE 4 TWO-WAVELENGTH INTERFACE BLOCK DIAGRAM

the event and until backscatter conditions regained the pre-event values. Prior to, or following, the scheduled events for a day the Mark IX lidar would perform and record a standard system calibration using calibrated optical attenuations. The Mark IX receiver gain control gates are checked as part of this calibration procedure. The ASL lidar performed a similar calibration but used layers of low-density polyethylene sheets placed in the transmit beam to reduce the received reference signal return. By inserting multiple layers of polyethylene in equal amounts per step, a receiver linearity and dynamic range calibration can be made by comparing the changes with calibrated electrical attenuations. The calibration example shown in Figure 5 is an example of a typical calibration recorded on a strip chart. The calibration is also digitally recorded on magnetic tape. The electrical calibration on the left is performed by inserting electrical step attenuations between the receiver detector and post-detector electronics, while the attenuation steps on the right are produced by the transmit beam attenuation method. Since the electrical calibration can be performed very easily, a calibration was generally recorded either before or after each event when the reference signal represented clear-air conditions.

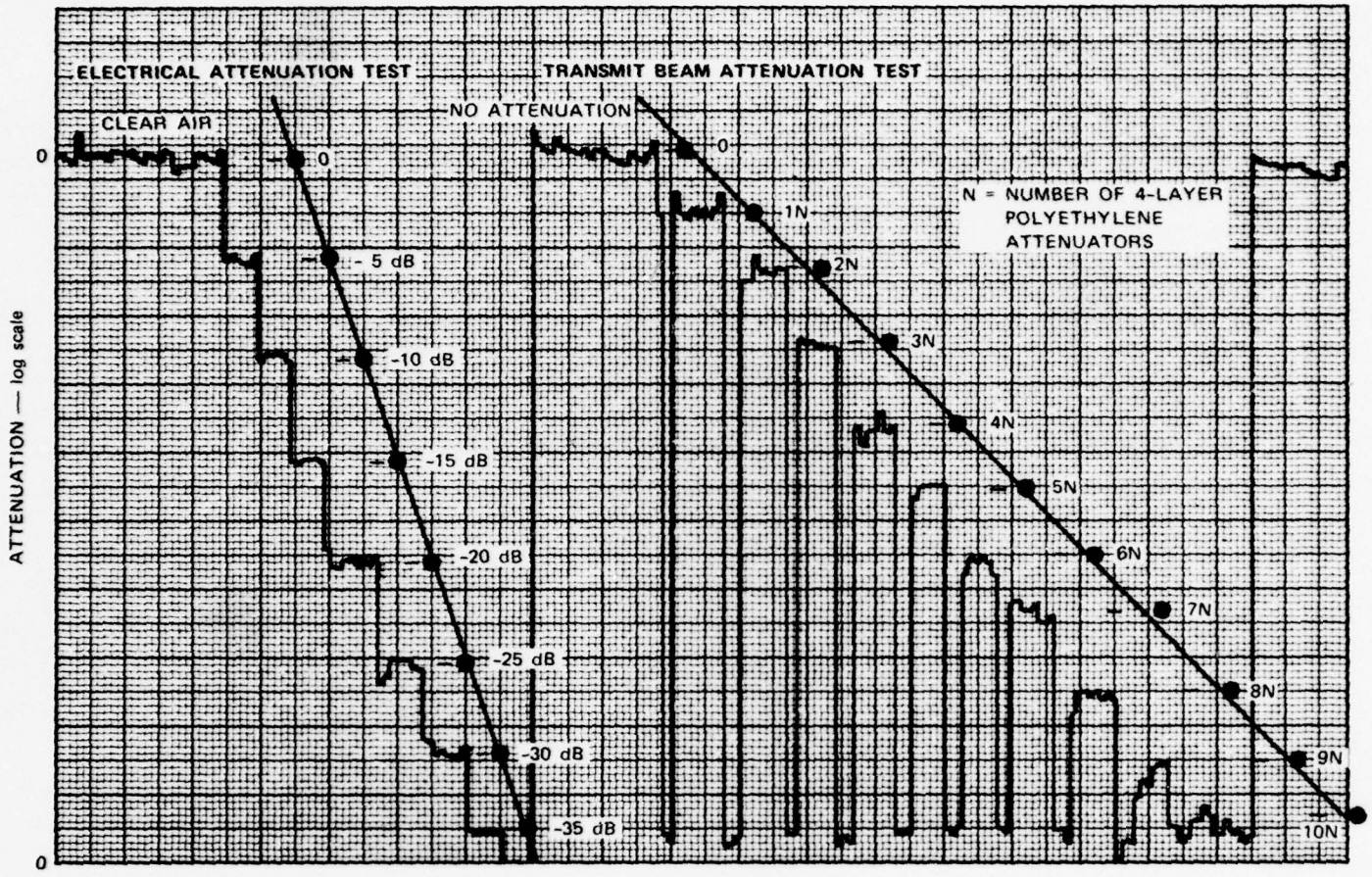

FIGURE 5 ASL LIDAR CALIBRATION DATA

IV DATA INVENTORY

The lidar data collected during the DIRT-I program are in several different formats as follows:

0.7 μm and 10.6 μm Digitized Backscatter Data--These primary two-wavelength data were recorded on magnetic tape for all events following the two-system interface on October 5, 1978. Prior to the system interface only 0.7-μm data are available on tape; no tape data are available for the A1-A4 test series as the Mark IX did not arrive on site until October 2, 1978. It should be noted that at some point between October 10 and 13 a digitizer problem developed in the Mark IX digitizer, degrading the amplitude resolution of digital data going onto tape. The problem was traced to a faulty tri-state semiconductor device controlling the "32"-weighted bit output and is the cause of the poor resolution evident in the October 13 data presented in Appendix A. The problem was solved prior to recording the October 14 data (Appendix B) by using the ASL transient recorder digital output card.

10.6 μm Strip Chart Data--This data (energy output and target return amplitude) exist for all events in linear and log-amplitude strip chart format. The strip chart data have been digitized using a hand-trace digitizer so that the data can be computer-processed. Examples of the strip chart and digitized computer-processed data are shown in Figure 6. The upper trace on the strip chart data is an example of typical 10.6 μm energy variations during a data run ($< \pm 5\%$). The lower strip chart record is an actual event (A-4) of target signal amplitude variations. The computer-processed transmission plot shown in Figure 6b was derived from the digitized strip chart data.

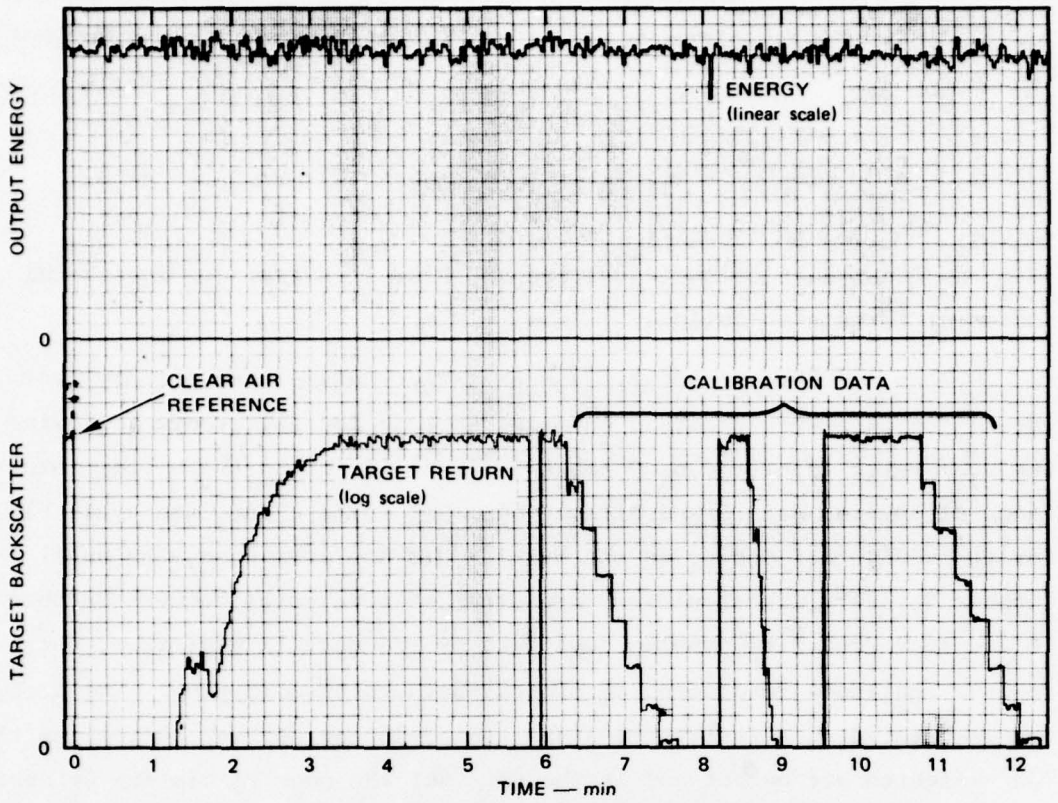

(a) TWO CHANNEL STRIP CHART DATA

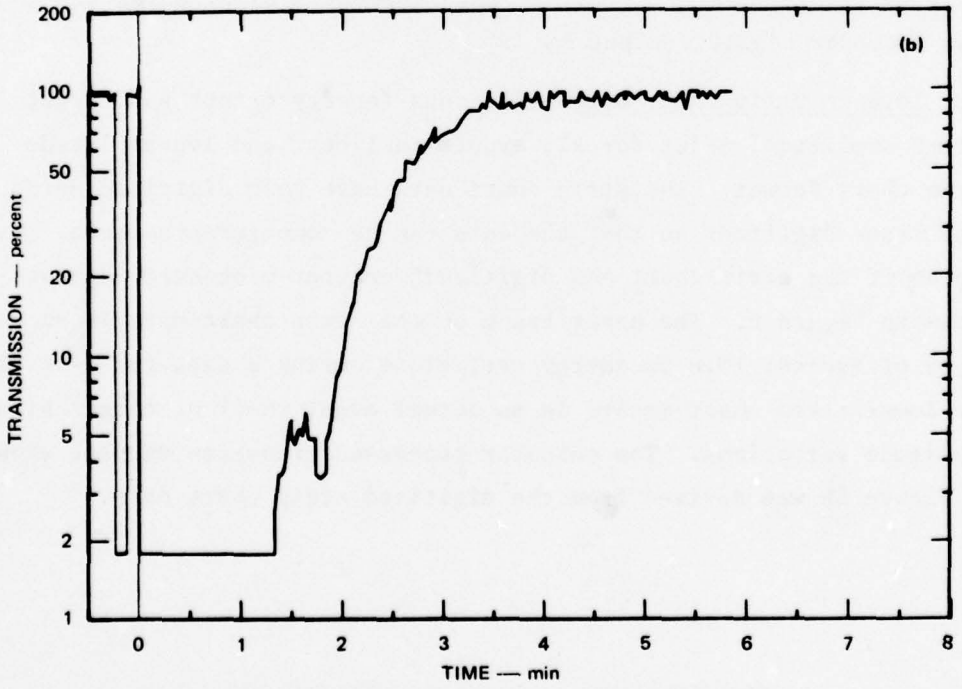

(b) COMPUTER PROCESSED DIGITIZED STRIP CHART DATA

FIGURE 6 ASL LIDAR DATA EXAMPLES (A-4 Event)

10.6 μm Range-Resolved Backscatter Photographs--A polaroid photograph sequence of 10.6 μm backscatter data is available for each event, with the exception of D1-D4 and F1-F4 when the ASL digitizer developed problems. Examples of the range-resolved backscatter sequences are presented in this report (in the discussion of data analysis in Section V) along with transmission plots to aid in understanding transmission changes taking place and to observe cloud structure during the events.

Table 2 is an inventory and summary of data collected during the DIRT-I program.

In addition to the above data, TV video records (video tape) of the lidar optical path were made during each event. A review of this data during data analysis provides helpful information about conditions such as wind direction and evidence of smoke in the test zone.

Table 2

LIDAR DATA INVENTORY

Date	Event	Data*					Comments
		1	2	3	4	5	
Oct. 2	A-1	X	✓	✓	✓	✓	X = not available;
	A-2	X	✓	✓	✓	✓	Mark IX not on site
	A-3	X	✓	✓	✓	✓	
	A-4	X	✓	✓	✓	✓	✓ = data available
Oct. 3	B-1	+	✓	✓	✓	✓	+ = 0.7 μm data only;
	B-2	+	✓	✓	✓	✓	two-wavelength inter-
	B-3	+	✓	✓	✓	✓	face not complete
	B-4	+	✓	✓	✓	✓	
	B-5	+	✓	✓	✓	✓	
	B-6	+	✓	✓	✓	✓	
	B-7	+	✓	✓	✓	✓	
	B-8	+	✓	✓	✓	✓	
Oct. 5	C-1	✓	✓	✓	✓	✓	
Oct. 6	D-1	✓	✓	✓	✓	X	X = not available;
	D-2	✓	✓	✓	✓	X	ASL lidar digitizer
	D-3	✓	✓	✓	✓	X	malfunction
	D-4	✓	✓	✓	✓	X	
Oct. 10	C-2	✓	✓	✓	✓	✓	
Oct. 11	E-1	✓	✓	✓	✓	✓	
	E-2	✓	✓	✓	✓	✓	
	E-3	✓	✓	✓	✓	✓	
	E-4	✓	✓	✓	✓	✓	
Oct. 12	F-1	✓	✓	✓	✓	X	X = not available
	F-2	✓	✓	✓	✓	X	ASL lidar digitizer
	F-3	✓	✓	✓	✓	X	malfunction
	F-4	-X	-X	-X	-X	-X	-X (F-4) = live 155
Oct. 13	F-5	✓	✓	✓	✓	✓	mm rounds missed test
	F-6	✓	✓	✓	✓	✓	zone
	F-7	✓	✓	✓	✓	✓	
	F-8	✓	✓	✓	✓	✓	
Oct. 14	E-5	✓	✓	✓	✓	✓	
	E-6	✓	✓	✓	✓	✓	
	E-7	✓	✓	✓	✓	✓	
	E-8	✓	✓	✓	✓	✓	
	E-9	✓	✓	✓	✓	✓	
	E-10	✓	✓	✓	✓	✓	
Oct. 14	G-1	✓	✓	X	✓	✓	

* 1. Digitized 0.7 and 10.6 μm range-resolved backscatter data; 9-track magnetic tape.
2. 10.6 μm target return amplitude data; strip chart recordings.
3. 10.6 μm digitized target return data; IBM card/tape format.
4. 10.6 μm energy output; strip chart recordings.
5. 10.6 μm range-resolved backscatter; (A-scope) photographs; polaroid sequence.

V DATA PROCESSING AND ANALYSIS

A. Processing

Two-Wavelength Data--The digitized two-wavelength lidar data taken during the DIRT-I program provides the most useful lidar information obtained because it can be processed to provide a variety of information. In this report we have processed the data to provide transmission comparisons between the two wavelengths, but other information such as comparisons of range-resolved backscatter, optical depth, peak backscatter, plume opacity, or profiles of relative plume density can also be derived. As already stated, the primary purpose of this program was the evaluation of the capabilities of the ASL lidar system for observations of dense smoke and dust and not a quantitative evaluation of cloud density.

In order to obtain transmission information from the backscatter target returns, a calibration relating the receiver light input to digitizer output must be derived for both wavelengths. The calibration procedures discussed in Section IV provide this information.

In general, the Mark IX receiver is well characterized with respect to laser energy backscattered by the atmosphere and passive reflective targets, and only occasional calibrations are required. However, because two wavelengths are involved and several different interface configurations were evaluated during the DIRT-I program, a separate calibration was performed each day. Moreover, the problem of nonlinearity in response to the high-amplitude reference target signal, as observed during the Dugway program, can be compensated for with daily calibrations. This was not a problem during the DIRT-I program because more operational time was available to characterize the response. There is no nonlinear response observed in the 10.6 μm data as indicated by the calibration record shown in Figure 5.

Having established the two-wavelength system response characteristics, transmission values are derived by comparing the signal return,

as a function of time, with respect to an average value obtained during the pre-test (clear air) conditions. Since the data is recorded logarithmically, the data must first be linearized before performing the averaging function on the clear-air values. The transmission values derived in this manner experience two-way path loss attenuation so that the apparent transmission losses must be divided by two (2) when displaying single-pass transmission values. Visible and infrared transmission plots are shown later in this section and Appendices A and B.

B. Analysis

Analysis of the two-wavelength lidar data presented in Appendices A and B indicate that, with the exception of events C-2, F-7, and G-1, little difference in transmission is observed. The data are surprisingly consistent regarding recovery times, and the various two-wavelength transmission feature changes (cloud density variations) track very closely. This suggests that the slight differences in sample time (0.5 sec) and optical path (approximately 2 m in test zone) do not represent a significant problem in measurements of dust clouds. The lack of wavelength dependence in the measurements indicates that the particle size distribution in the generated dust clouds at White Sands is quite broad and that a rather substantial proportion of large particles ($\approx$10 μm) exists. This is consistent with preliminary size distribution measurements[3] made during two events (F-6 and C-1) of the DIRT-I program. The two dust events that indicate a noticeable transmission difference are the C-2 and F-7 events, and they are addressed in detail in the following discussions. Also, the oil/rubber fire event (G-1) will be discussed.

C-2--October 10, 1978--This event was one of two large-scale detonations where 140-TNT charges were fired simultaneously in a uniformly-distributed array covering a substantial area of the test zone. A major reason for the large coverage was to minimize the effect of wind direction on the results.

The 10.6 μm backscatter record at time zero (T=0) in Figure 7 shows that a clear air backscatter signature exists; that is, only atmospheric scatter and the scatter from the reference beam-stop target at 2 km are observed along the lidar path. The small return seen at 100 m is off-axis reflection from a reflector placed there to provide a range mark reference. The corresponding time on the transmission plot shown in Figure 8 indicates a value greater than 100% for the 10 μm data and less than 100% for the 0.7 μm data which, of course, cannot be the case. The reason for this anomaly is that the pre-event backgraound data could not be used in this case to establish the transmission reference signal because the detonation shock wave altered the lidar optical alignments. For this reason, post-event conditions were used to establish the transmission reference, and data before T=0 should be ignored. At T+2 (Figure 7) complete blockage of the 2-km target signal is observed and is caused by the extremely dense dust cloud in the test zone. The very sharp pulse at approximately 900-m range indicates that there is little penetration into the cloud by the laser pulse. By T+30 s stratified cloud structure can be seen in front of the main cloud, but the main cloud density still blocks any penetration. This condition continues in examples T+1 min and T+2 min, and it appears that the very dense cloud structure is either growing in size or moving in the direction of the lidar. By T+3 min the cloud density along the lidar path is reduced such that the target return is now observed, and density structure can be observed on the back side of the cloud. It is also obvious that the cloud is moving toward the lidar instrumentation area. The transmission plot (Figure 8) shows that both wavelengths appear to recover from total transmission outage at the same time, but by T+3 min (and through T+15 min) there is a definite transmission difference between the 10.6-μm and 0.7-μm wavelengths. The remaining backscatter records, T+4 through T+16 min, illustrate the lidar's ability to track dust cloud movements and, in this case, the cloud drifts in the direction of the lidar and through the instrumentation area.

From the lidar data presented here it would appear that there is indeed a wavelength-dependent mechanism present in the dust cloud generated in this event. However, since only one other dust event (E-7,

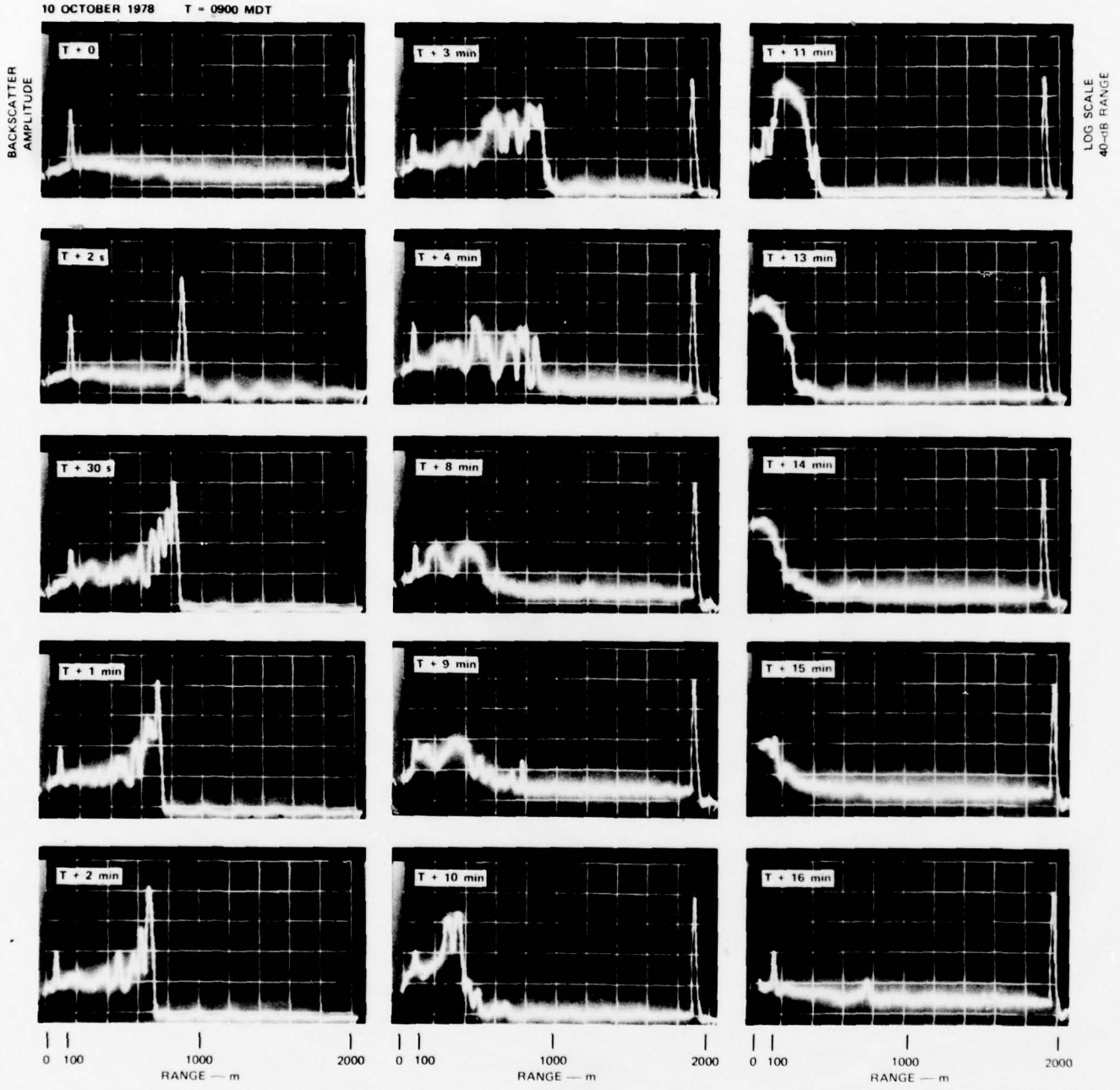

FIGURE 7 EVENT C-2 10.6-μm BACKSCATTER DATA

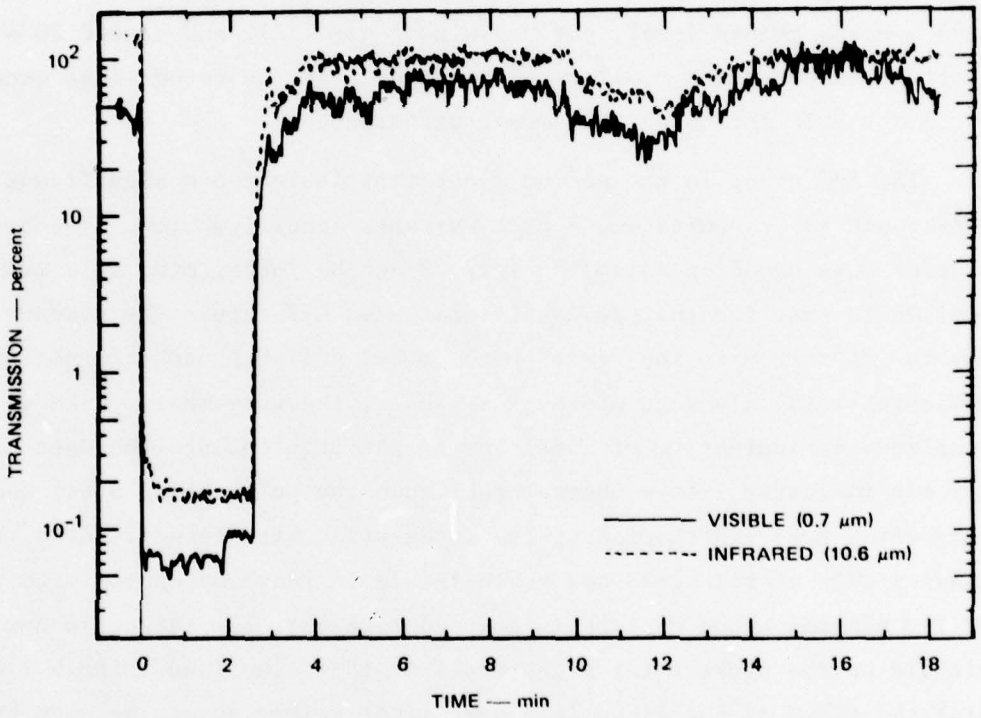

FIGURE 8 EVENT C-2 TWO-WAVELENGTH TRANSMISSION

discussed below) indicates any significant difference in transmission the C-2 data was re-evaluated several times for possible errors. No measurement or processing errors were discovered, but a review of the TV observations (which also include recorded voice comments) indicates that a large amount of smoke was generated during this event and is probably the wavelength-dependent mechanism responsible for the apparent anomaly with respect to the other data.

E-7--October 14, 1978--This event consisted of three statically-detonated, 155-mm howitzer rounds slanted at a 30^{o} angle to the vertical, 0.03 m below ground level, covered with loose fill, and placed 20 m apart. The event was similar to the other E-series detonations except for minor orientation and placement differences.

The E-7 event is the second event that indicated a significant difference in transmission, and it warrants special review. The backscatter data sequence shown in Figure 9 can be interpreted in a manner similar to that for the previously-discussed C-2 data. The absence of any target return in the first photo at T+2 s (T=0 photograph not taken) indicates total blockage of the laser beam; the very sharp pulse in the test zone is indicative of little or no penetration into the dust cloud. T+1 min indicates little change other than the pulse being a bit wider, indicating some penetration (pulse integration with range). Also, the leading edge of the cloud has moved inward in range by approximately 100 m. By T+3 min the cloud density is reduced such that the target is now visible on the backscatter signature. At this time (and through T+4 min) the cloud is contained in a very tight volume as can be seen by the lack of irregular density structure in the cloud. This, however, does not imply that there are not fine density variations within the cloud; however, within the range resolution capability of the 10.6 μm lidar (30 m) the structure appears rather uniform. Within this time frame (+3 to +4 minutes) the transmission difference between 0.7 μm and 10.6 μm is significant, as seen in Figure 10. The transmission plot shows that both wavelengths start to recover from total outage at the same time and both exhibit the same general recovery shape. The 10.6-μm transmission, however, is measurably greater during this period. After T+4 min the

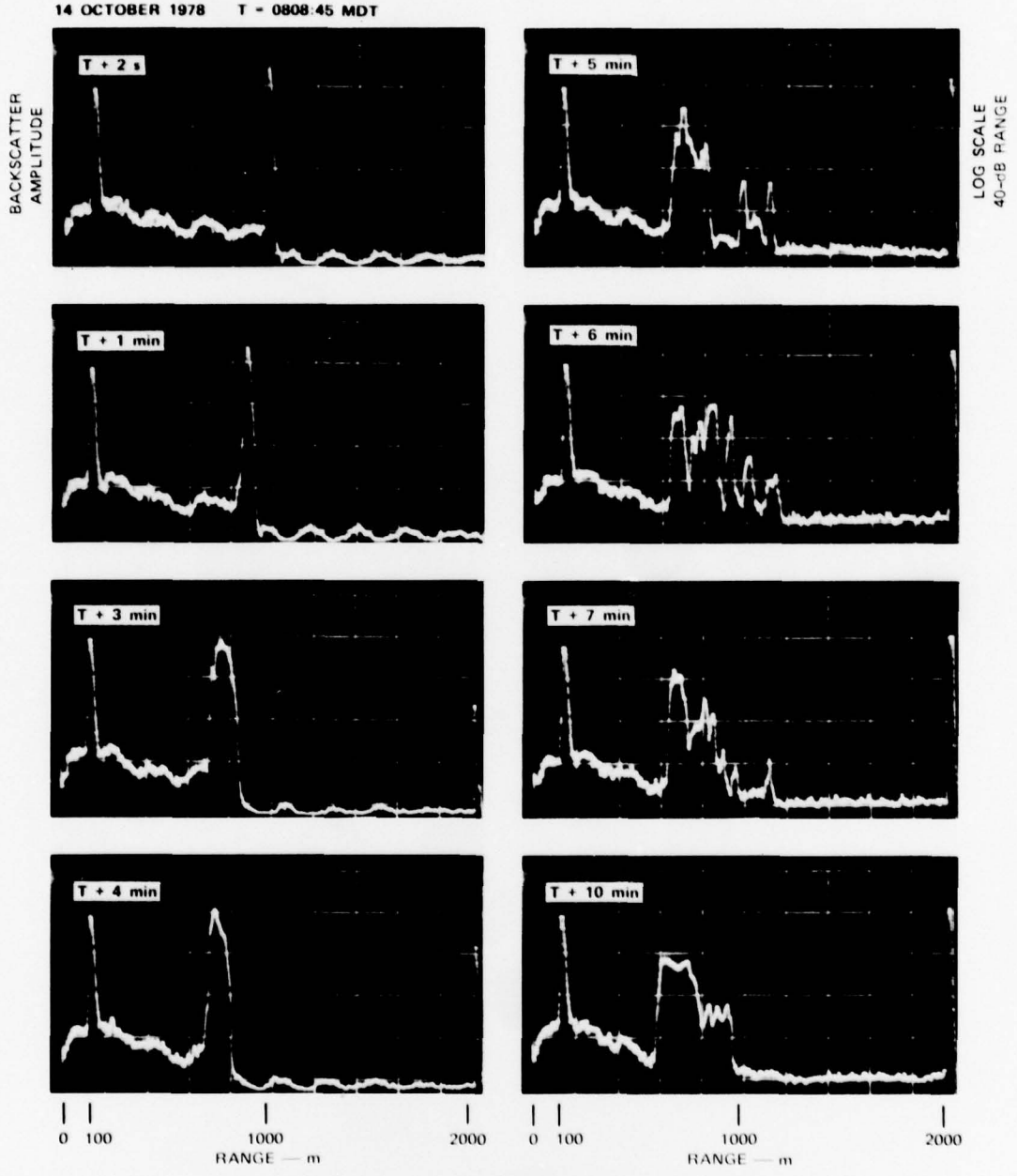

FIGURE 9 EVENT E-7 10.6-μm BACKSCATTER DATA

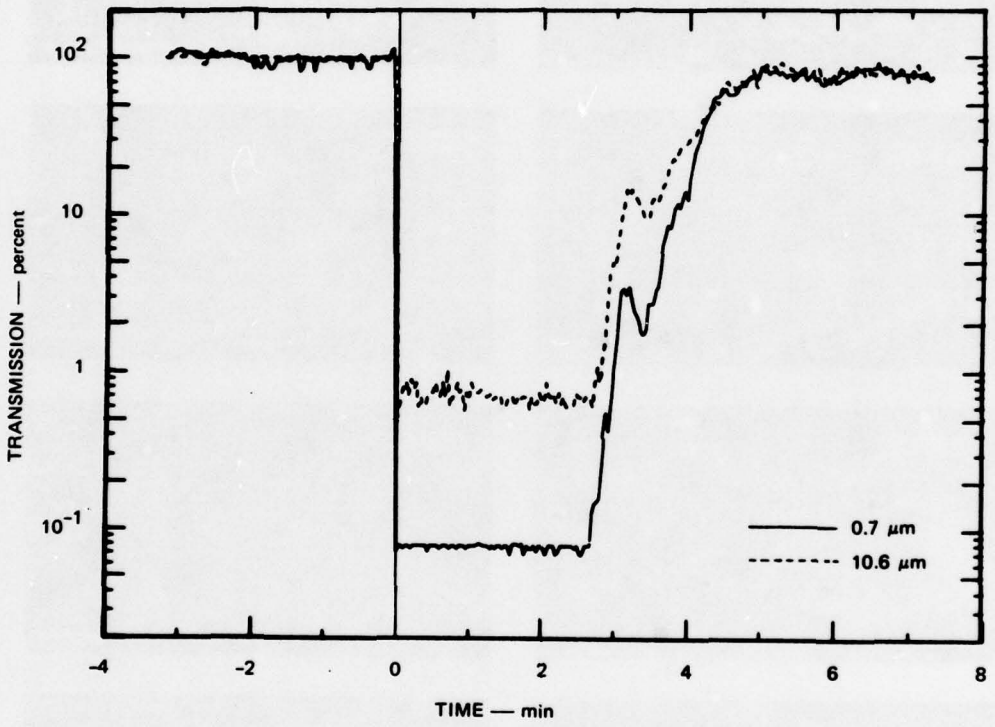

FIGURE 10 EVENT E-7 TWO-WAVELENGTH TRANSMISSION

cloud begins to break up, as seen in the remaining backscatter photographs, and transmission continues to recover. The difference in transmissions between 0.7 μm and 10.6 μm disappears after T+4 min which indicates that the integrated attenuations of the multiple-plume cloud structure is not wavelength-dependent. From an evaluation of the data between T+3 and T+4 min more closely, and a review of the TV recordings of the event, it is quite evident that the wind in the test zone during the event could be responsible for the transmission difference if there are fine density variations within the cloud. Another possible explanation is that wavelength-dependent smoke generated along with the dust cloud is present during that time frame. A more careful look at other E-series events (Appendix B) indicates that there is a small but similar anomaly during the transmission recovery in several of the events.

G-1--Oil/Rubber Fire--The last event in the DIRT-I program was a diesel fuel, oil, and rubber fire burning from a trench in the center of the test zone. Large volumes of black smoke were produced for a period of approximately 37 min, but due to the variable wind conditions, the plumes of smoke moved intermittently in and out of the lidar optical path. Total blockage of the 0.7-μm transmission was observed quite often as the plumes crossed the optical path as seen in the transmission plot (Figure 11). The transmission plot also shows that the 10.6 μm transmission was never totally blocked. The backscatter record, which represents the maximum attenuation observed and is also shown in Figure 11, was calibrated after the event in clear-air conditions and found to represent 12.2 dB attenuation (about 6% transmission). This large wavelength differential is similar to previous smoke test data results which were explained by relating aerosol extinction at the two wavelengths to particle size distribution. Use of the same analogy would suggest that the smoke generated in the DIRT-I event was primarily of small particle-size particulates. However, preliminary particle size distribution data[3] for the event indicates that the particle size distribution is similar to that measured during the dust events where no wavelength dependence is observed. Resolution of this anomaly will require an analysis beyond the scope of this report and will require a knowledge of the refractive indices and absorption coefficients of the smoke particulates.

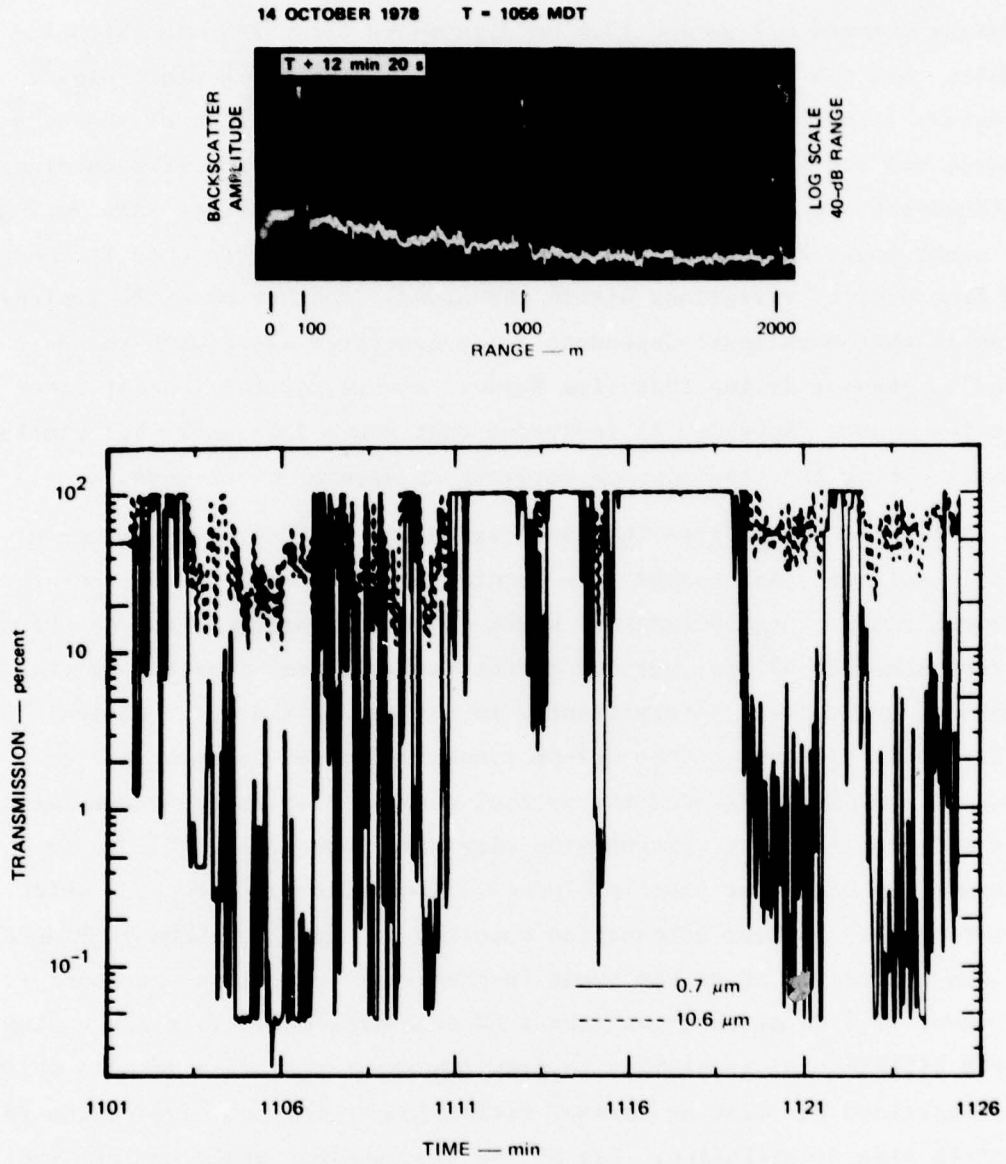

FIGURE 11 EVENT G-1 10.6-μm BACKSCATTER DATA AND TWO-WAVELENGTH TRANSMISSION

VI CONCLUSIONS AND RECOMMENDATIONS

A. Conclusions

Results of the DIRT-I program indicate that the broad particle size distribution present in the dust generated at White Sands produces little if any wavelength-dependent transmission effects. The few observed exceptions, where greater 10.6-μm transmission is indicated, generally can be explained by the presence of wavelength-dependent smoke along the optical path, which is also generated by the detonations. Backscatter-to-transmission relationships are grossly related but, in general, are quite nonlinear, as can be expected when multiple and specular scatter by the large, irregular-shaped particles, as well as strong attenuation, are involved. The oil/rubber fire generated dense black smoke that was totally opaque to the 0.7-μm lidar, while the 10.6 μm transmission measurements indicate a "worse-case" transmission of approximately 6%.

B. Recommendations

The following suggestions for further ASL lidar system improvements to develop an optimum lidar system for remote observations of dense dust and smoke result from system evaluation during DIRT-I.

(1) The ASL lidar should incorporate recording capability and some field evaluation processing capability that can be upgraded as required.

(2) Multiwavelength operation of the ASL lidar should be adopted. The Nd:YAG laser would be a logical choice for the second wavelength because of current military interest in the 1.06 μm wavelength. Other wavelengths, such as 3 μm, should be considered in future expansion.

(3) Angular scanning should be implemented; use of the LDV scanning system is a possibility.

(4) The TV observations during the DIRT-I program provided a very useful processing and operational aid and should be adopted as part of the system.

(5) Suggested ASL system operational improvements involve the following components:

The HgCdTe photodiode detector/amplifier which should be modified for dc coupled operation to prevent coupling capacitor charge build-up causing negative overshoot in data.

The ASL log amplifier which should be modified to provide a lower frequency response. The current 1 kHz low-frequency response should be lowered to 10 Hz to prevent large-amplitude, wide-pulse inputs from causing overshoot that forces the log amplifier through zero.

The transmit/receive mirror which should be modified for finer and more stable control.

Finally, general van renovation should be performed to improve lighting, air conditioning, and ac distribution. The van is also in need of weather stripping and painting.

REFERENCES

1. J. E. van der Laan, "A System Description of an Improved 10.6 μm Lidar System for Monostatic Optical Measurements of Battlefield Dust and Smoke," Technical Report No. 2, ARO Contract DAAG29-77-C-0001, SRI Project 5862 (1979).

2. E. E. Uthe, "Lidar Observations of Smoke and Dust Clouds at 0.7-μm and 10.6-μm Wavelengths," Technical Report No. 1, ARO Contract DAAG29-77-C-0001, SRI Project 5862 (1978).

3. James D. Lindberg, "Measured Effects of Battlefield Dust and Smoke on Visible, Infrared, and Millimeter Wavelength Propagation: A Preliminary Report on Dusty Infrared Test-I (DIRT-I)," ASL Technical Report No. 0021, DA Task No. 1L161102B53A-13 (1979).

4. E. E. Uthe and R. J. Allen, "A Digital Real-Time Lidar Data Recording, Processing, and Display System, Optical and Quantum Electronics, Vol. 7, pp. 121-129 (1975).

APPENDIX A

DIRT-I DATA EVENTS F-5, 6, 7, 8

(October 13, 1978)

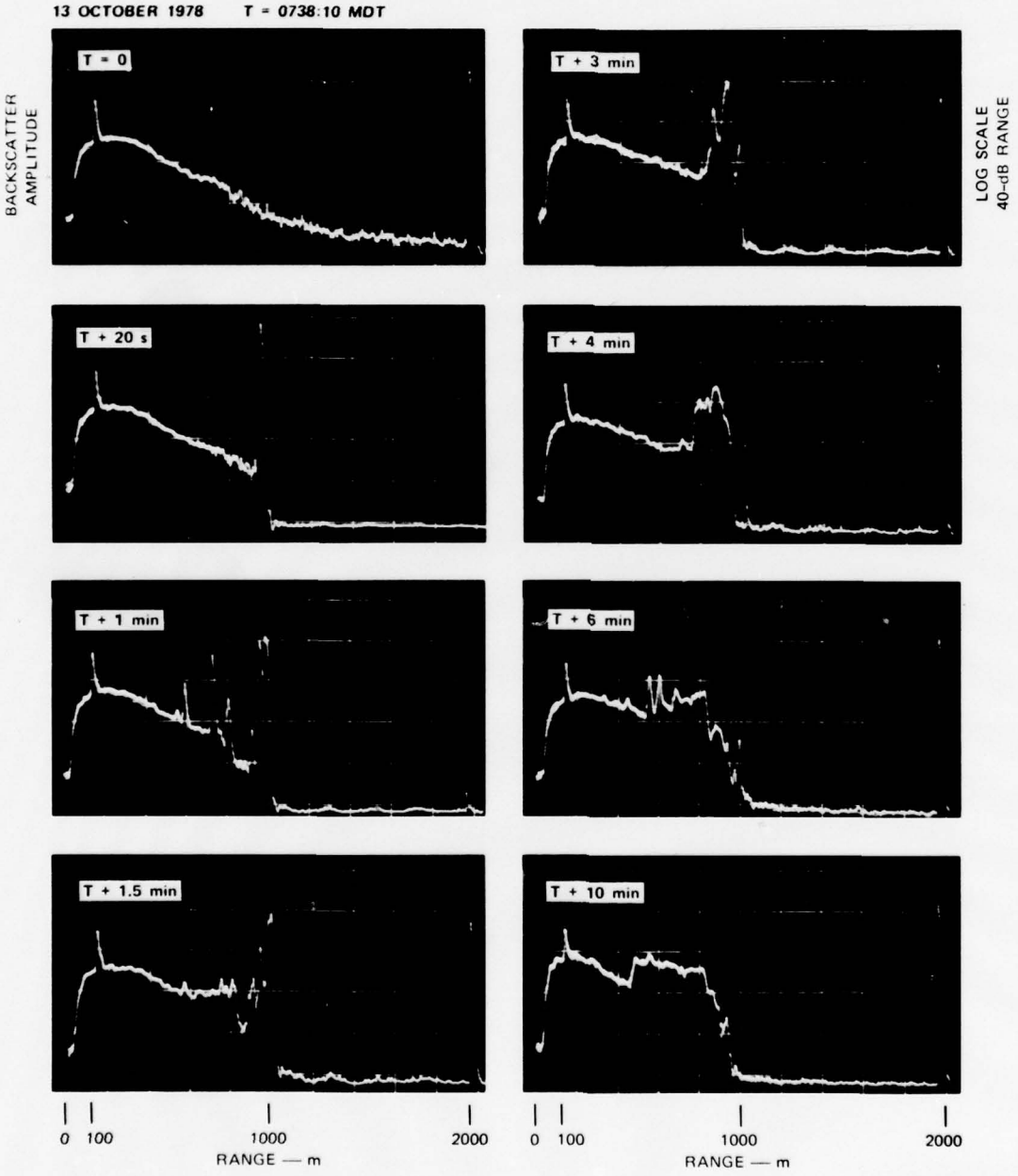

FIGURE A-1 EVENT F-5 10.6-μm BACKSCATTER DATA

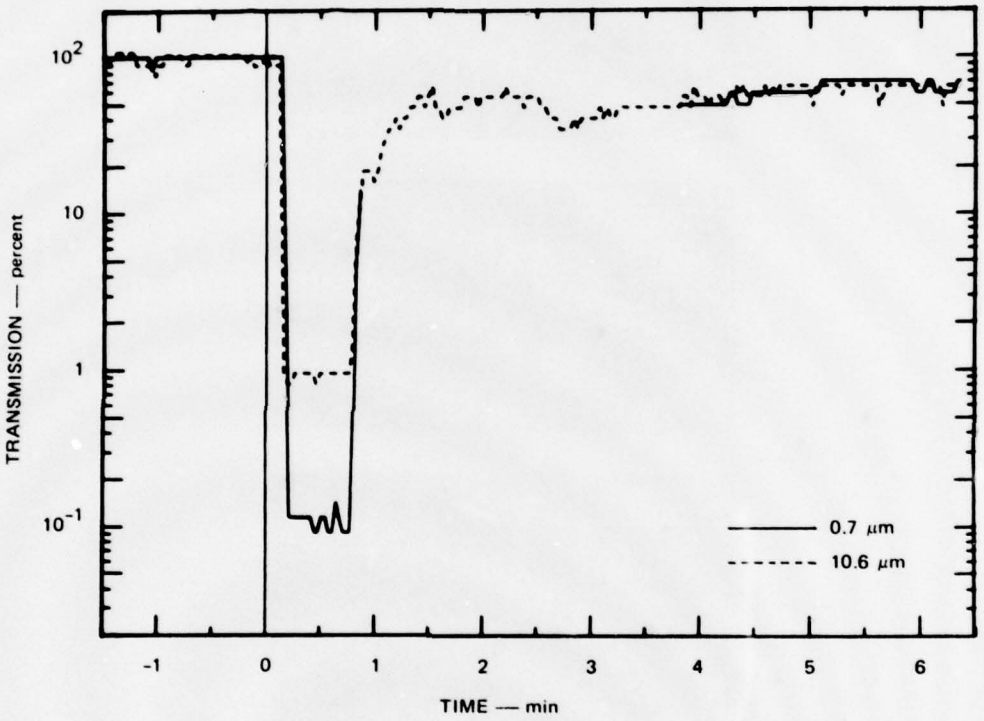

FIGURE A-2 EVENT F-5 TRANSMISSION DATA

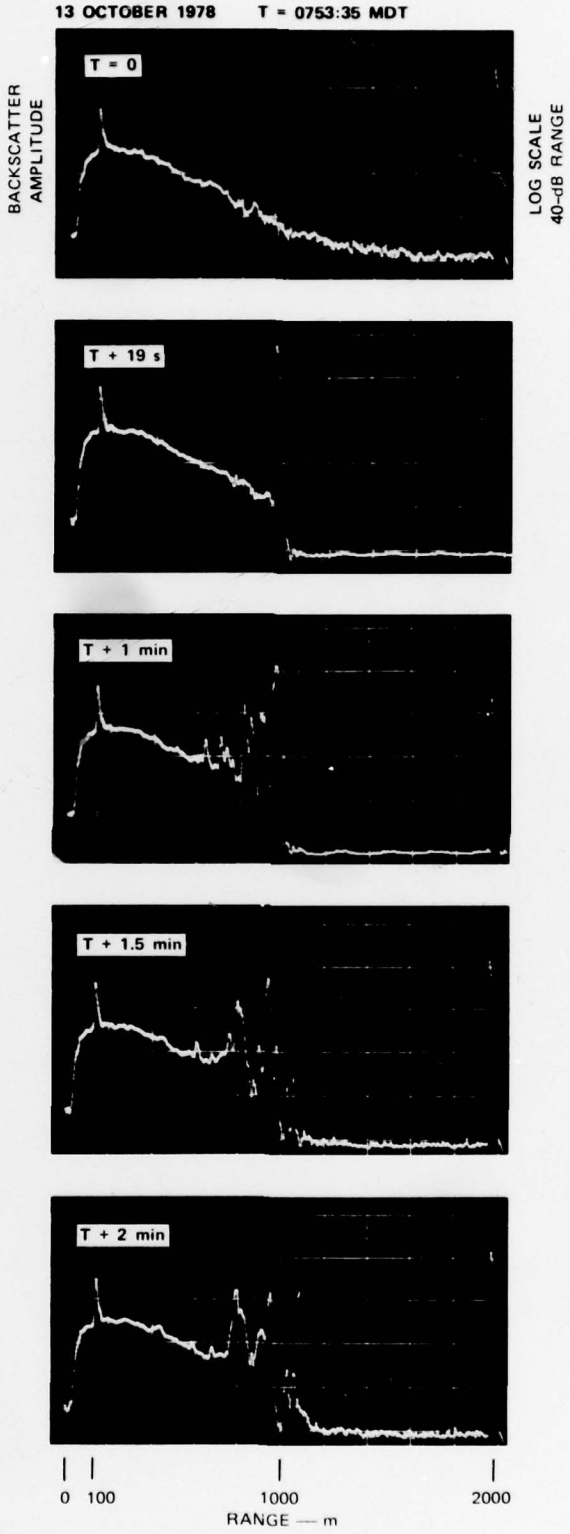

FIGURE A-3 EVENT F-6 10.6-μm BACKSCATTER DATA

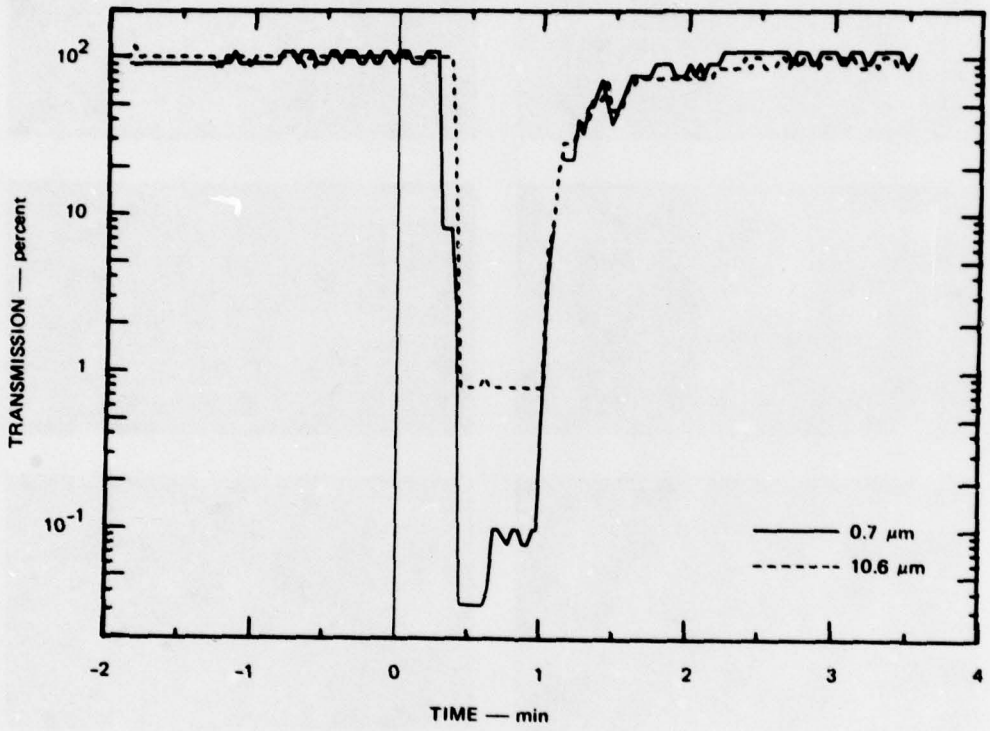

FIGURE A-4 EVENT F-6 TRANSMISSION DATA

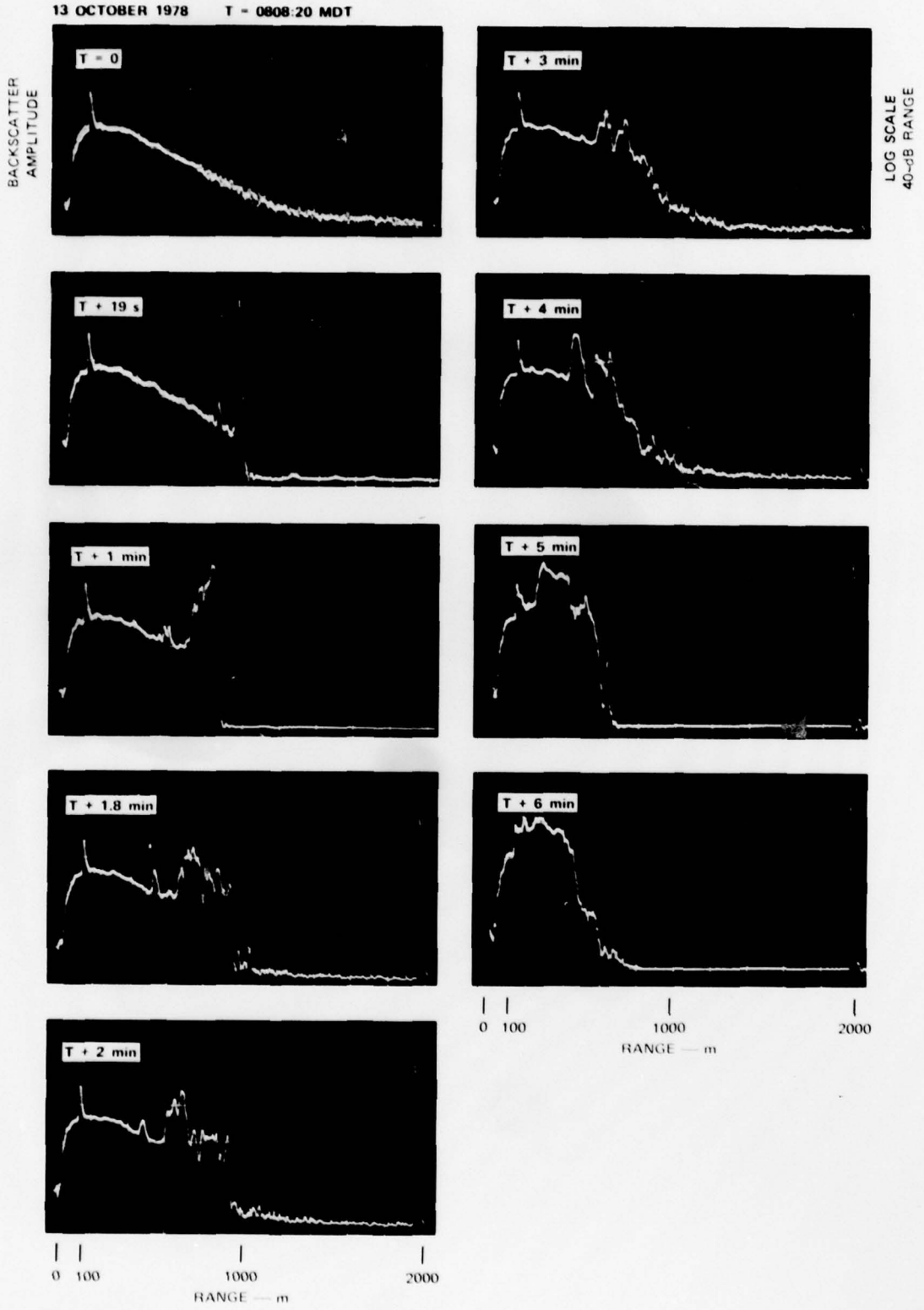

FIGURE A-5 EVENT F-7 10.6-μm BACKSCATTER DATA

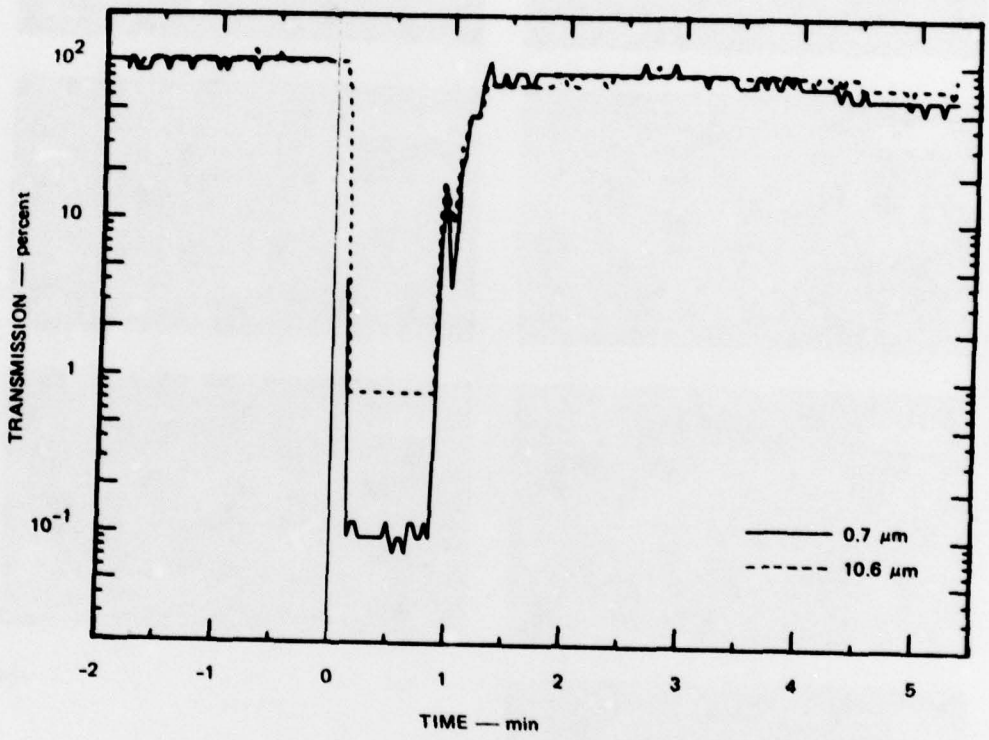

FIGURE A-6 EVENT F-7 TRANSMISSION DATA

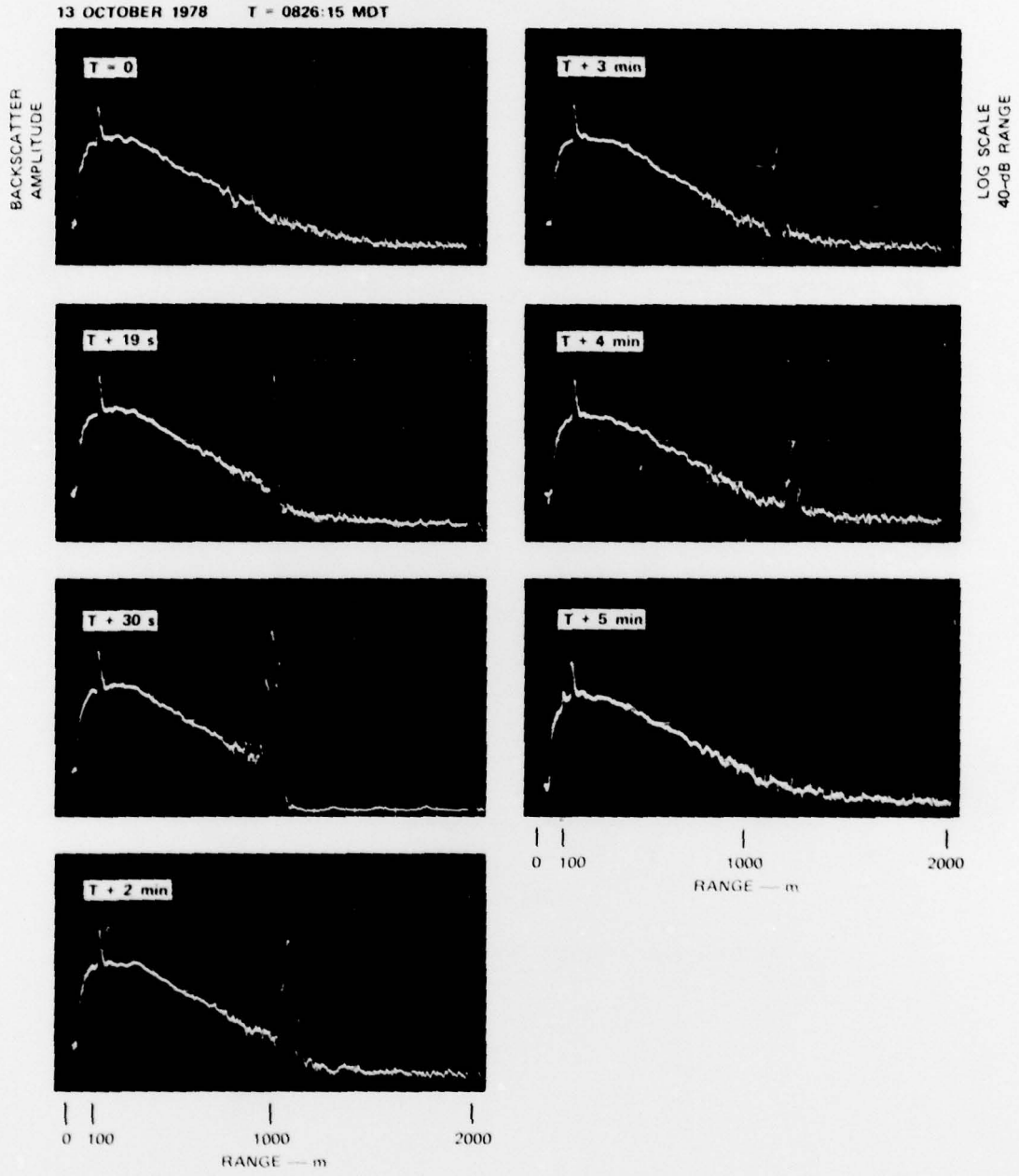

FIGURE A-7 EVENT F-8 10.6-μm BACKSCATTER DATA

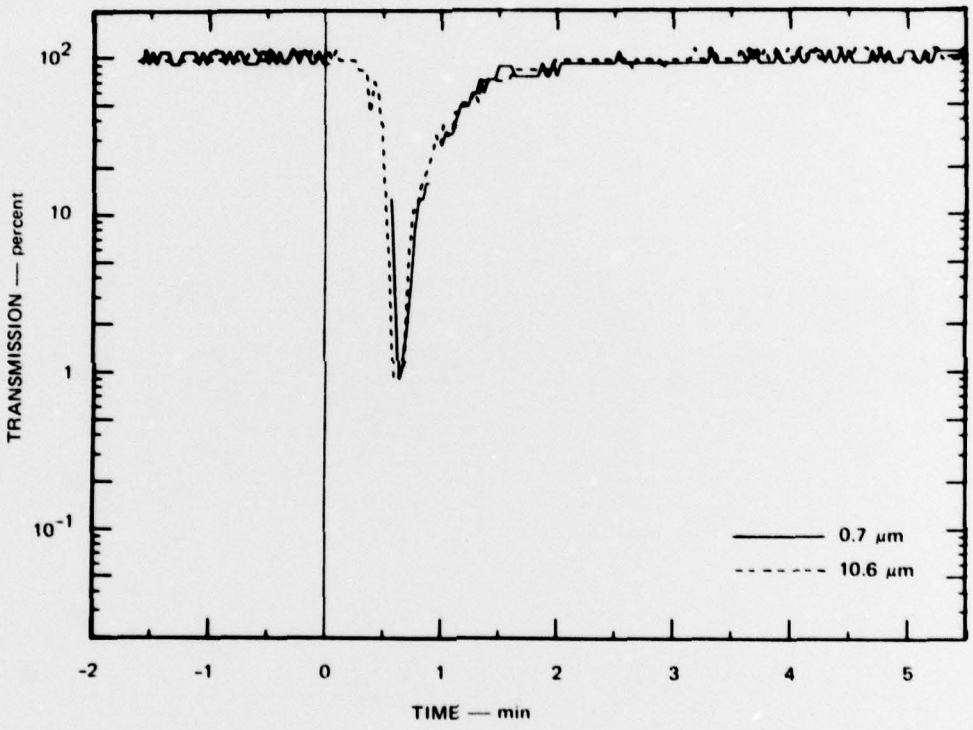

FIGURE A-8 EVENT F-8 TRANSMISSION DATA

APPENDIX B

DIRT-I DATA EVENTS E-5, 6, 8, 9, 10

(October 14, 1978)

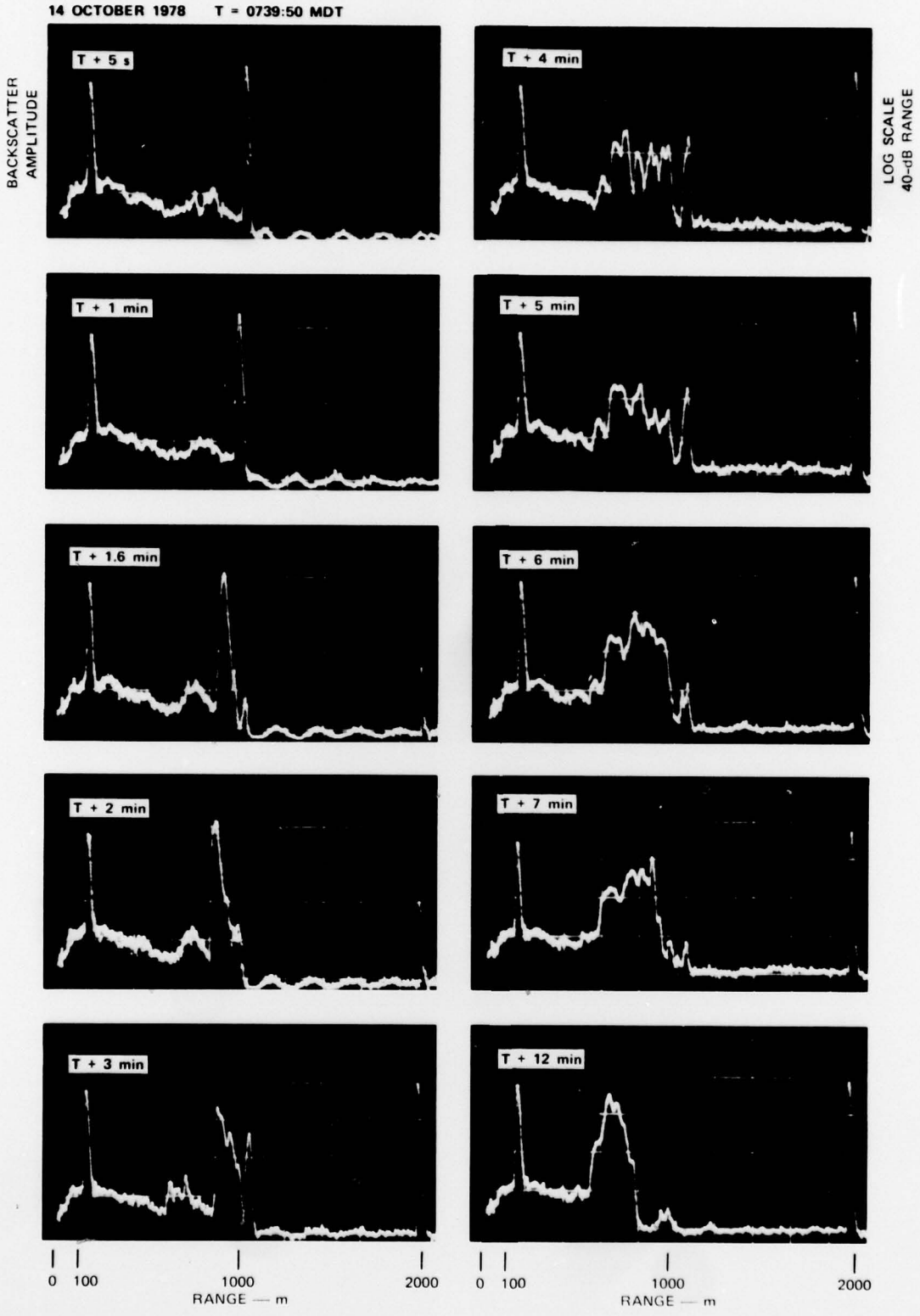

FIGURE B-1 EVENT E-5 10.6-μm BACKSCATTER DATA

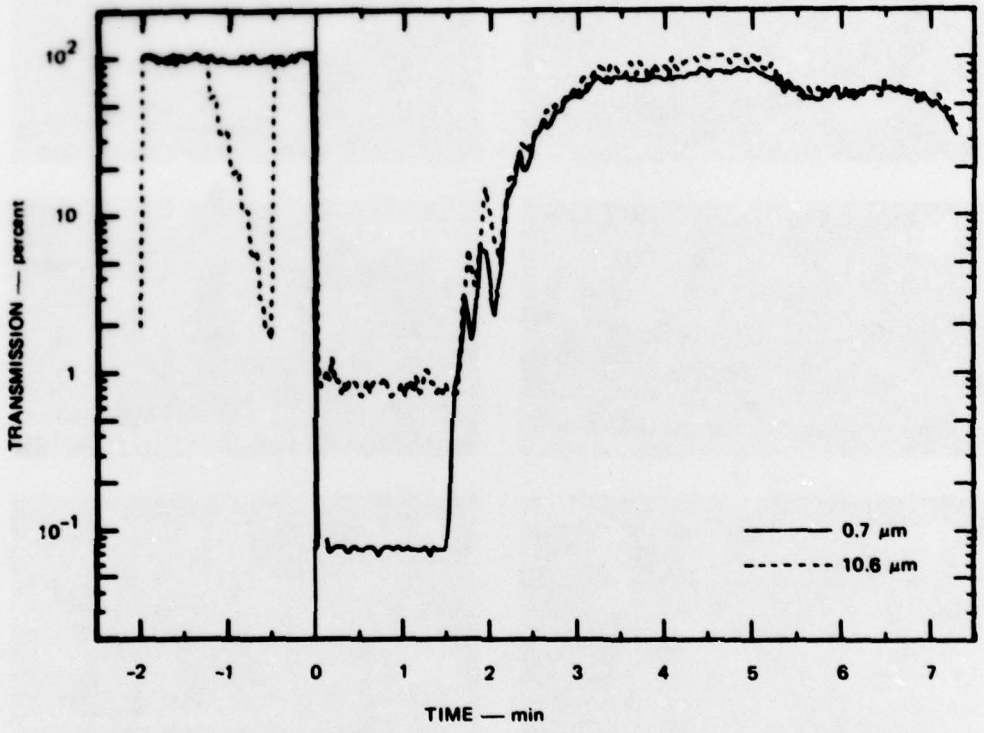

FIGURE B-2 EVENT E-5 TRANSMISSION DATA

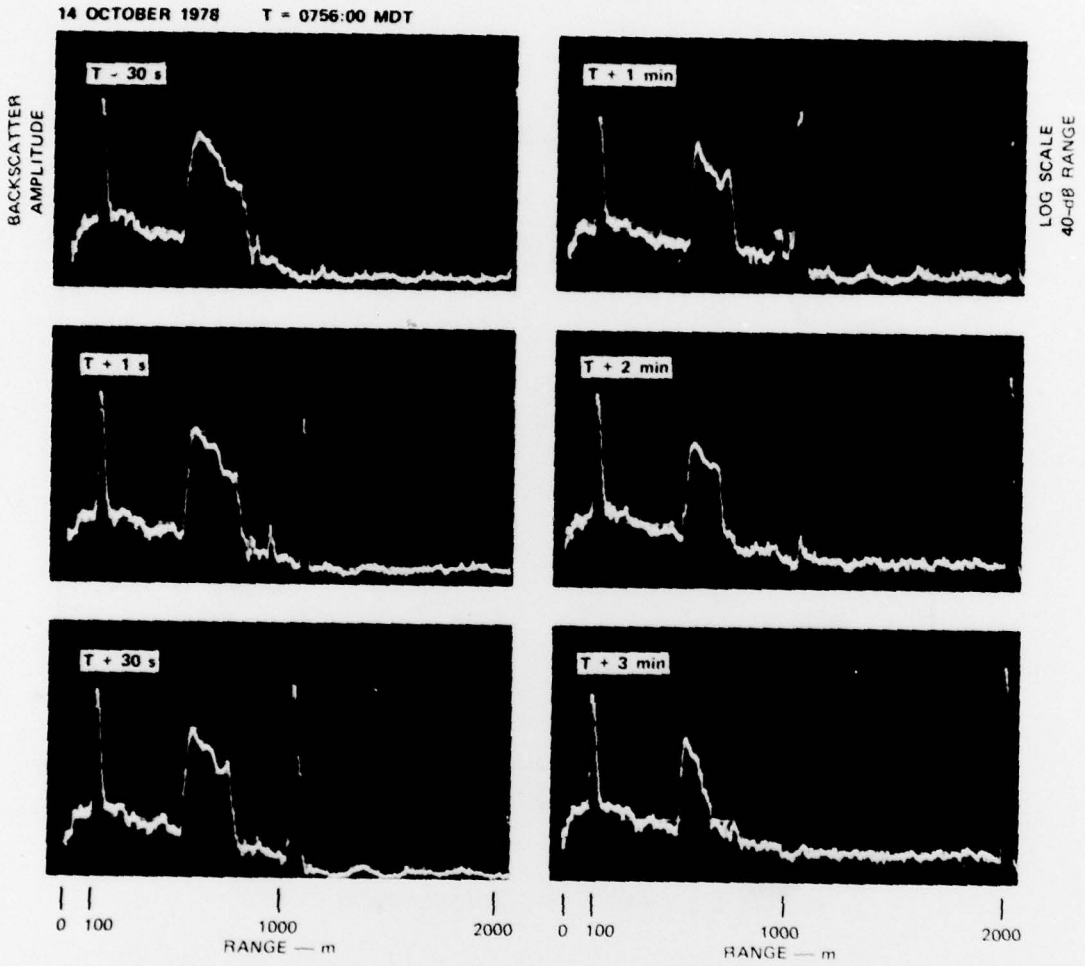

FIGURE B-3 EVENT E-6 10.6-μm BACKSCATTER DATA

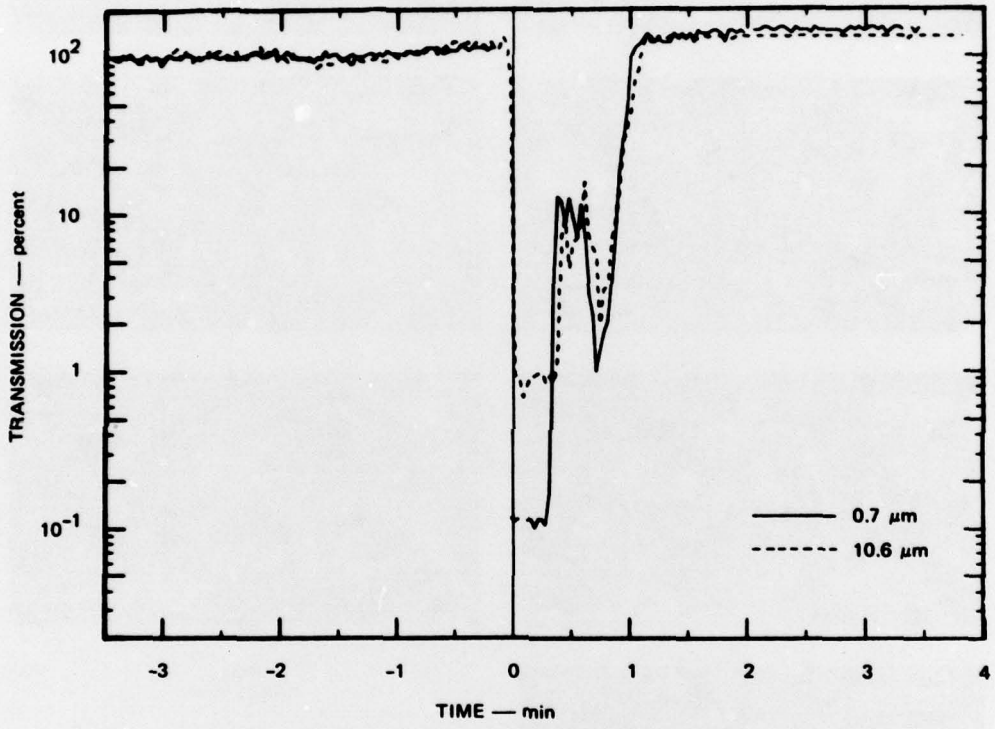

FIGURE B-4 EVENT E-6 TRANSMISSION DATA

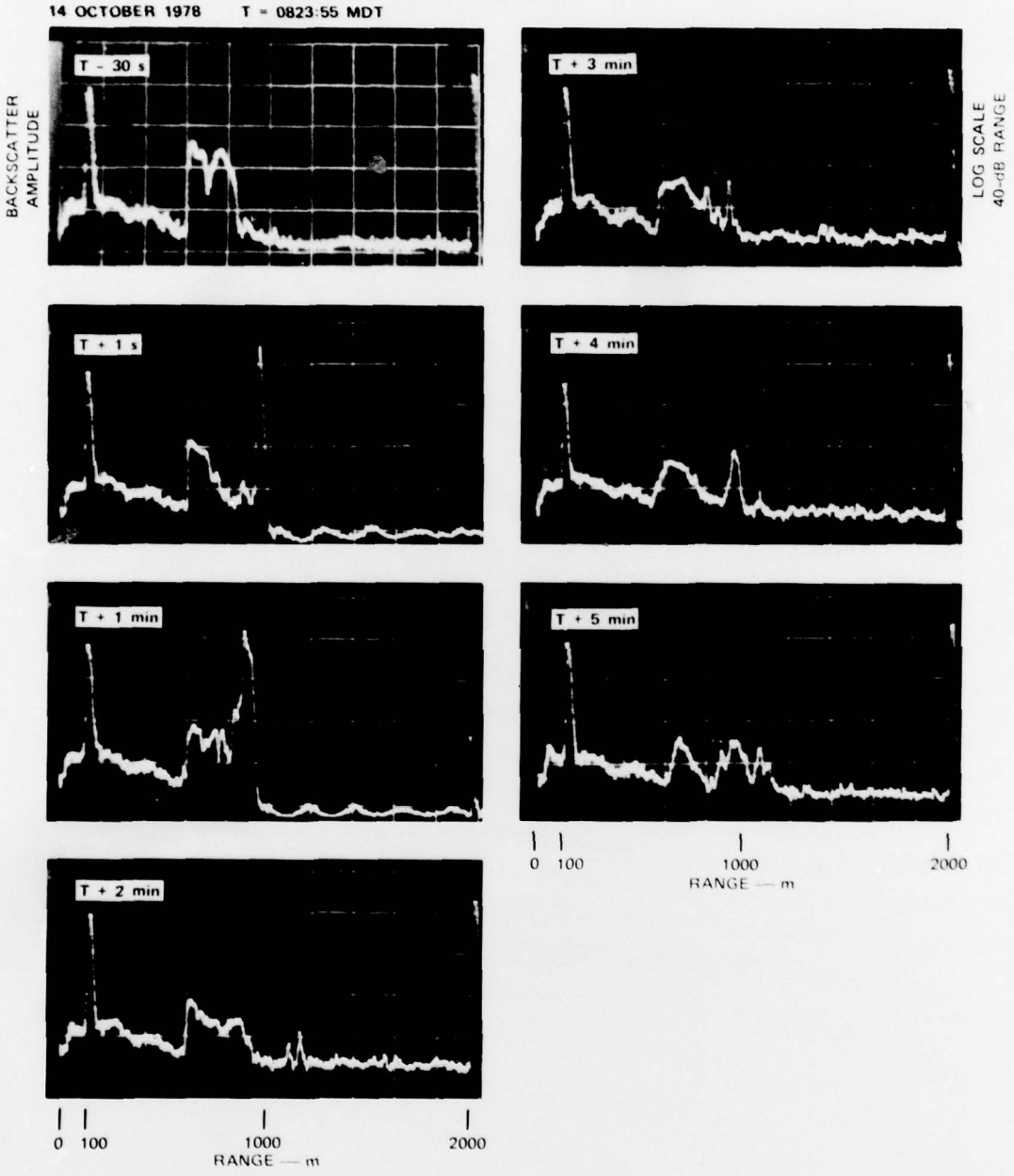

FIGURE B-5 EVENT E-8 10.6-μm BACKSCATTER DATA

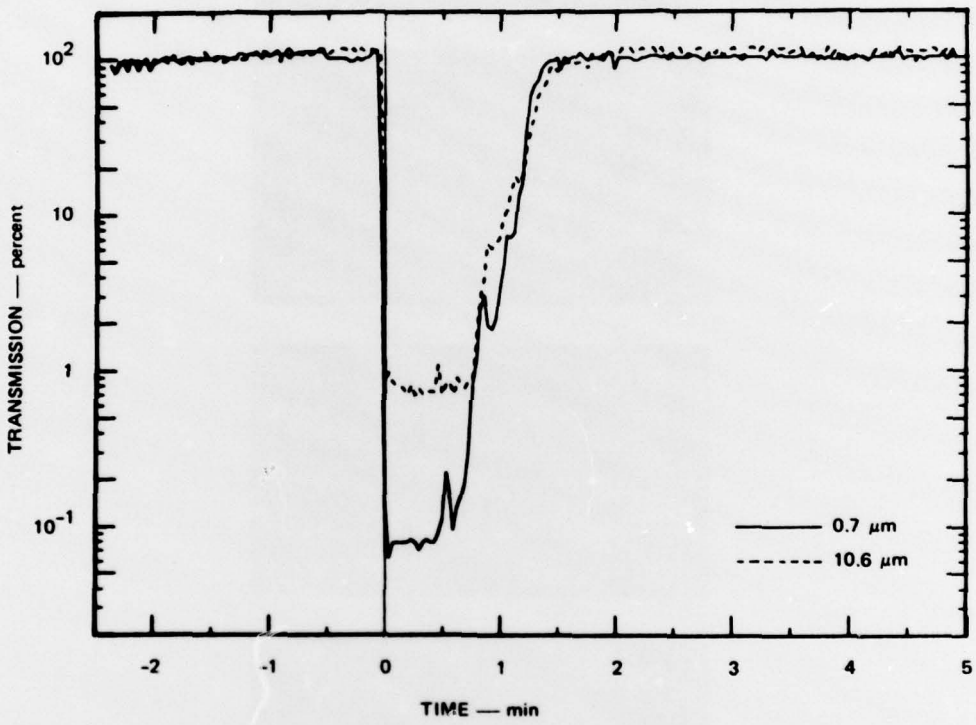

FIGURE B-6 EVENT E-8 TRANSMISSION DATA

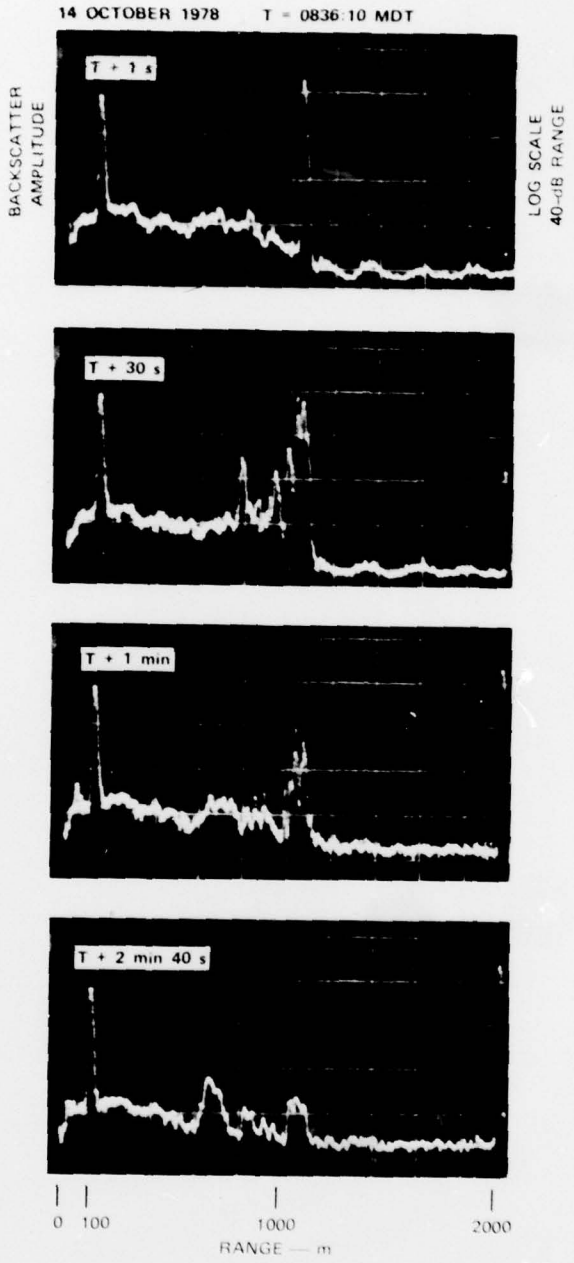

FIGURE B-7 EVENT E-9 10.6-μm BACKSCATTER DATA

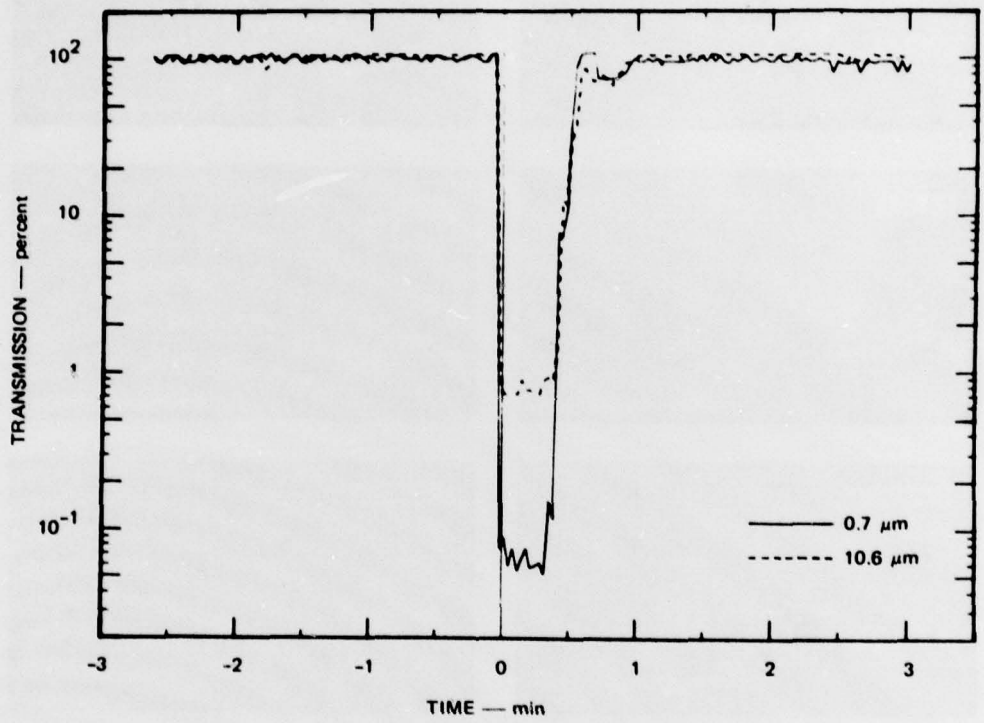

FIGURE B-8 EVENT E-9 TRANSMISSION DATA

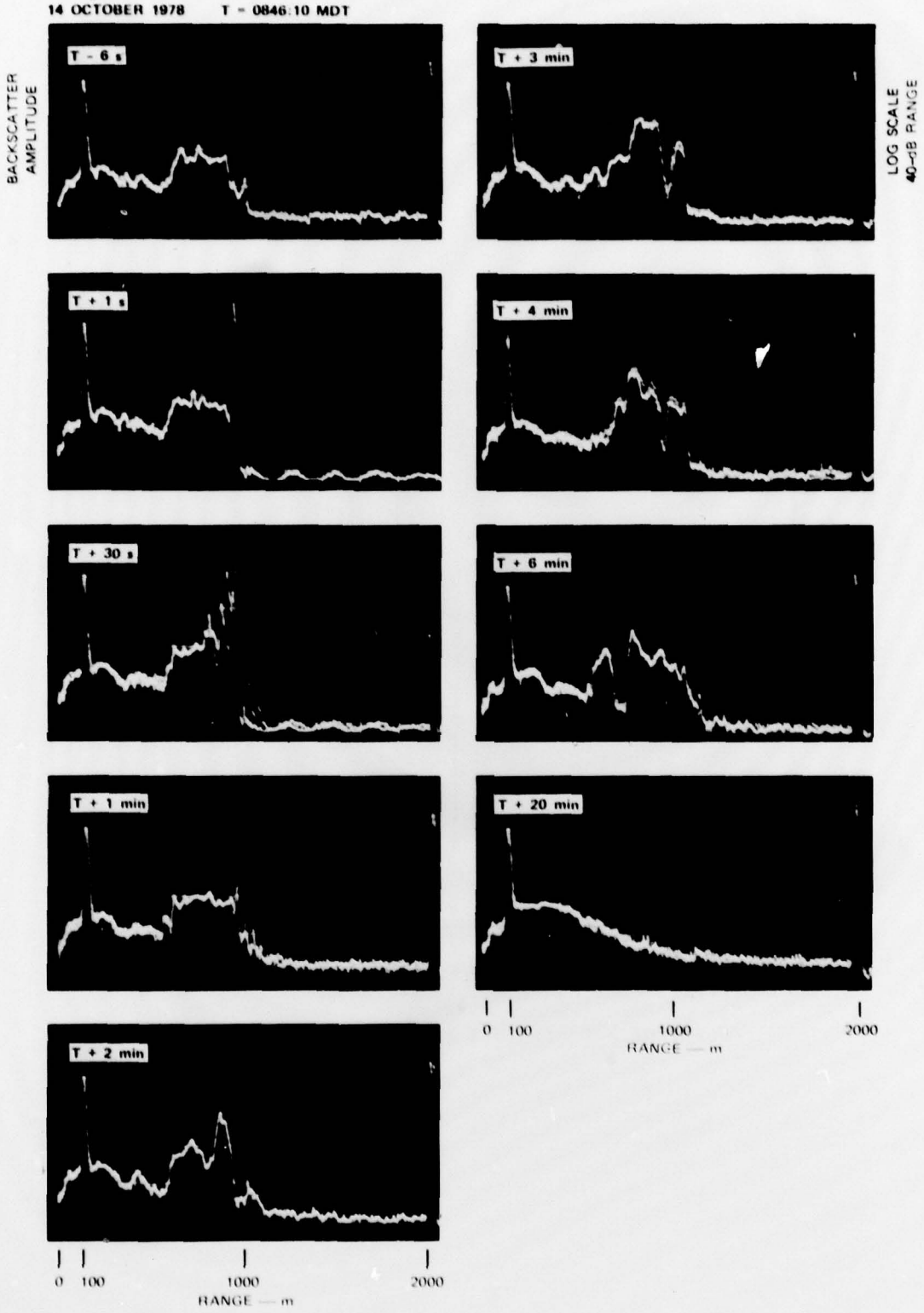

FIGURE B-9 EVENT E-10 10.6-μm BACKSCATTER DATA

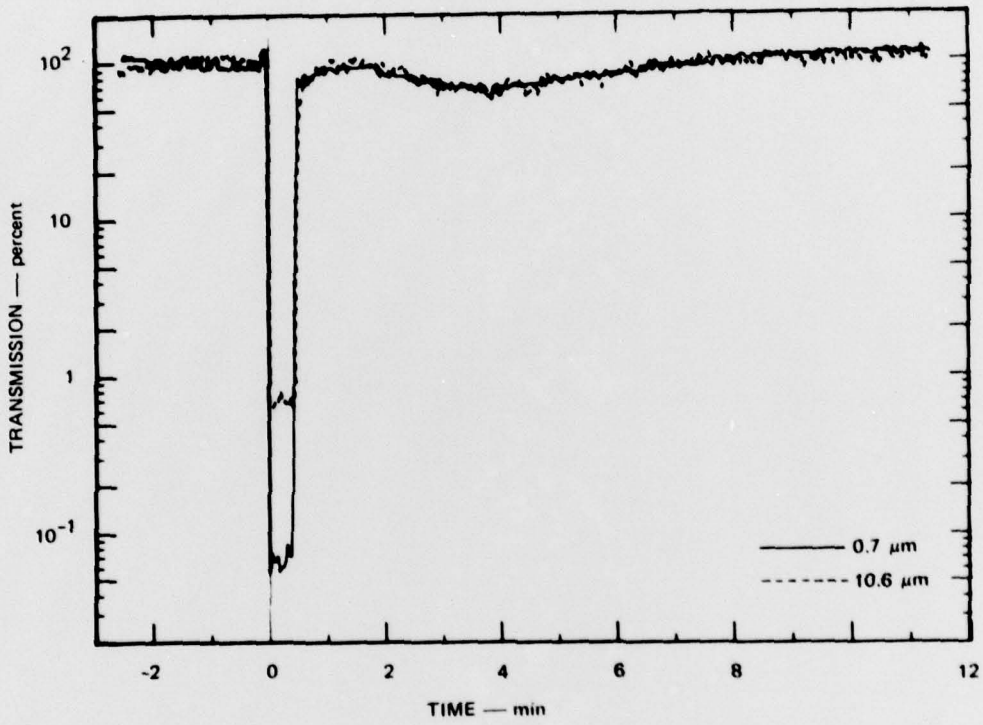

FIGURE B-10 EVENT E-10 TRANSMISSION DATA